

# DRV8231A 3.7-A Brushed DC Motor Driver with Integrated Current Sense and Regulation

## 1 Features

- N-channel H-bridge brushed DC motor driver
- 4.5-V to 33-V operating supply voltage range
- Pin-to-pin,  $R_{DS(on)}$ , voltage, and current sense/regulation variants (external shunt resistor and integrated current mirror)
  - DRV8870: 6.5-V to 45-V, 565-mΩ, shunt
  - DRV8251: 4.5-V to 48-V, 450-mΩ, shunt
  - DRV8251A: 4.5-V to 48-V, 450-mΩ, mirror
  - DRV8231: 4.5-V to 33-V, 600-mΩ, shunt
  - DRV8231A: 4.5-V to 33-V, 600-mΩ, mirror
- High output current capability: 3.7-A Peak
- PWM control interface
- Supports 1.8-V, 3.3-V, and 5-V logic inputs
- Integrated I<sup>2</sup>PROPI current sensing for stall detection and current regulation
- Low-power sleep mode
  - $<1\text{-}\mu\text{A}$  at  $V_{VM} = 24\text{-V}$ ,  $T_J = 25^\circ\text{C}$
- Small package and footprint
  - 8-Pin WSON with PowerPAD™,  $2.0 \times 2.0$  mm
  - 8-Pin HSOP with PowerPAD™,  $4.9 \times 6.0$  mm
- Integrated protection features
  - VM undervoltage lockout (UVLO)
  - Auto-retry overcurrent protection (OCP)
  - Thermal shutdown (TSD)

## 2 Applications

- Printers
- Vacuum robot
- Washer and dryer
- Coffee machine
- POS printer
- Electricity meter
- ATMs (Automated Teller Machines)
- Ventilators
- Surgical equipment
- Electronic hospital bed and bed control
- Fitness machine

## 3 Description

The DRV8231A device is an integrated motor driver with N-channel H-bridge, charge pump, current sense feedback, current regulation, and protection circuitry. The charge pump improves efficiency by supporting N-channel MOSFET half bridges and 100% duty cycle driving.

An internal current mirror architecture on the I<sup>2</sup>PROPI pin implements current sensing and regulation. This eliminates the need for a large power shunt resistor, saving board area and reducing system cost. The I<sup>2</sup>PROPI current-sense output allows a microcontroller to detect motor stall or changes in load conditions. The external voltage reference pin, VREF, determines the threshold of current regulation during start-up and stall events without interaction from a microcontroller.

A low-power sleep mode achieves ultra-low quiescent current draw by shutting down most of the internal circuitry. Internal protection features include supply undervoltage lockout, output overcurrent, and device overtemperature.

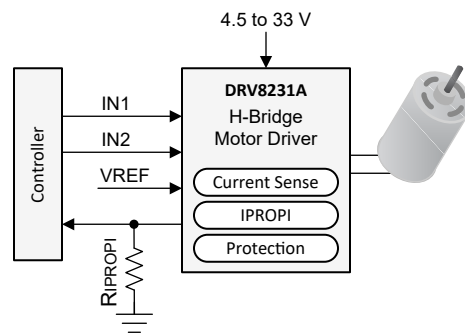
The DRV8231A is part of a family of devices which come in pin-to-pin, scalable  $R_{DS(on)}$  and supply voltage options to support various loads and supply rails with minimal design changes. See [Section 5](#) for information on the devices in this family. View the full portfolio of [brushed motor drivers](#) on [ti.com](#).

### Device Information <sup>(1)</sup>

PART NUMBER	PACKAGE	BODY SIZE (NOM)
DRV8231A	HSOP (8)	4.90 mm × 6.00 mm
	WSON (8)	2.00 mm × 2.00 mm

(1) For all available packages, see the orderable addendum at the end of the data sheet.

### Simplified Schematic



An IMPORTANT NOTICE at the end of this data sheet addresses availability, warranty, changes, use in safety-critical applications, intellectual property matters and other important disclaimers. PRODUCTION DATA.

## Table of Contents

<b>1 Features</b> .....	<b>1</b>	8.5 Device Functional Modes.....	<b>17</b>
<b>2 Applications</b> .....	<b>1</b>	8.6 Pin Diagrams.....	<b>18</b>
<b>3 Description</b> .....	<b>1</b>	<b>9 Application and Implementation</b> .....	<b>19</b>
<b>4 Revision History</b> .....	<b>2</b>	9.1 Application Information.....	<b>19</b>
<b>5 Device Comparison</b> .....	<b>3</b>	9.2 Typical Application.....	<b>19</b>
<b>6 Pin Configuration and Functions</b> .....	<b>3</b>	9.3 Current Capability and Thermal Performance.....	<b>26</b>
<b>7 Specifications</b> .....	<b>4</b>	<b>10 Power Supply Recommendations</b> .....	<b>32</b>
7.1 Absolute Maximum Ratings.....	4	10.1 Bulk Capacitance.....	32
7.2 ESD Ratings.....	4	<b>11 Layout</b> .....	<b>33</b>
7.3 Recommended Operating Conditions.....	4	11.1 Layout Guidelines.....	33
7.4 Thermal Information.....	4	11.2 Layout Example.....	33
7.5 Electrical Characteristics.....	5	<b>12 Device and Documentation Support</b> .....	<b>35</b>
7.6 Typical Characteristics.....	6	12.1 Documentation Support.....	35
7.7 Timing Diagrams.....	8	12.2 Receiving Notification of Documentation Updates.....	35
<b>8 Detailed Description</b> .....	<b>9</b>	12.3 Community Resources.....	35
8.1 Overview.....	9	12.4 Trademarks.....	35
8.2 Functional Block Diagram.....	9	<b>13 Mechanical, Packaging, and Orderable</b> <b>Information</b> .....	<b>35</b>
8.3 External Components.....	9		
8.4 Feature Description.....	11		

## 4 Revision History

NOTE: Page numbers for previous revisions may differ from page numbers in the current version.

DATE	REVISION	NOTES
November 2021	*	Initial Release

## 5 Device Comparison

**Table 5-1. Device Comparison Table**

Device name	Supply voltage (V)	R <sub>DS(on)</sub> (mΩ)	Current regulation	Current-sense feedback	Overcurrent protection response	Package	Pin-to-pin devices
DRV8870	6.5 to 45	565	External Shunt Resistor	External Amplifier	Automatic Retry	HSOP (4.9x6)	DRV8870, DRV8251, DRV8231
DRV8251	4.5 to 48	450			Latched Disable	HSOP (4.9x6)	
DRV8231	4.5 to 33	600			Automatic Retry	HSOP (4.9x6) WSON (2x2)	
DRV8251A	4.5 to 48	450	Internal current mirror (IPROPI)		Automatic Retry	HSOP (4.9x6)	DRV8251A, DRV8231A
DRV8231A	4.5 to 33	600			Automatic Retry	HSOP (4.9x6) WSON (2x2)	

## 6 Pin Configuration and Functions

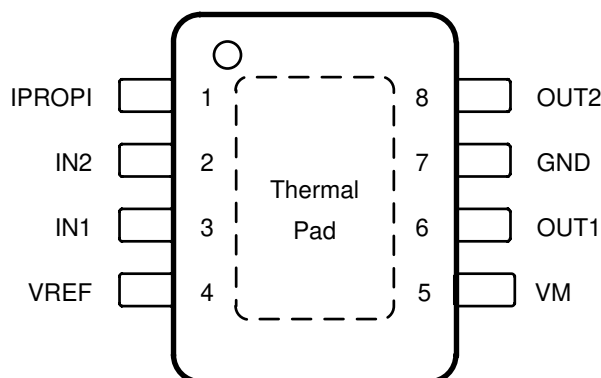


Figure 6-1. DDA Package 8-Pin HSOP Top View

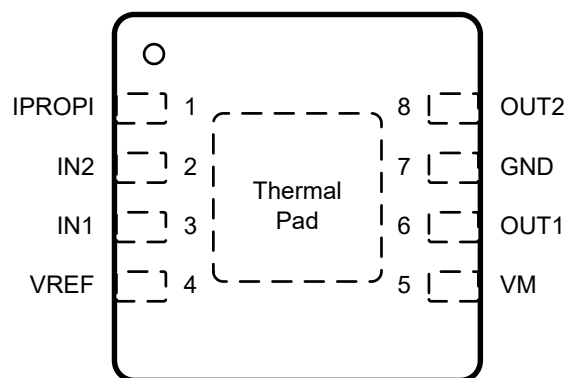


Figure 6-2. DSG Package 8-Pin HSOP Top View

**Table 6-1. Pin Functions**

PIN		TYPE	DESCRIPTION
NAME	NO.		
GND	7	PWR	Device power ground. Connect to system ground.
IN1	3	I	Logic inputs. Controls the H-bridge output. Has internal pulldowns. See <a href="#">Table 8-2</a> .
IN2	2	I	Logic inputs. Controls the H-bridge output. Has internal pulldowns. See <a href="#">Table 8-2</a> .
IPROPI	1	PWR	Analog current output proportional to load current. <a href="#">Section 8.4.2.1</a> .
OUT1	6	O	H-bridge output. Connect directly to the motor or other inductive load.
OUT2	8	O	H-bridge output. Connect directly to the motor or other inductive load.
VM	5	PWR	4.5-V to 48-V power supply. Connect a 0.1-µF bypass capacitor to ground, as well as sufficient bulk capacitance, rated for the VM voltage.
VREF	4	I	Analog input. Apply a voltage between 0 to 5 V. For information on current regulation, see the <a href="#">Section 8.4.2.1</a> section.
PAD		—	Thermal pad. Connect to board ground. For good thermal dissipation, use large ground planes on multiple layers, and multiple nearby vias connecting those planes.

## 7 Specifications

### 7.1 Absolute Maximum Ratings

over operating temperature range (unless otherwise noted)<sup>(1)</sup>

		MIN	MAX	UNIT
Power supply pin voltage	VM	-0.3	35	V
Power supply transient voltage ramp	VM	0	2	V/ $\mu$ s
Logic pin voltage	INx	-0.3	7	V
Reference input pin voltage	VREF	-0.3	6	V
Output pin voltage	OUTx	-0.7	VM + 0.7	V
Current sense input pin voltage	IPROPI	-0.3	5.75	V
Output current	OUTx	Internally Limited	Internally Limited	A
Junction temperature, T <sub>A</sub>	Junction temperature, T <sub>A</sub>	-40	125	°C
Junction temperature, T <sub>J</sub>		-40	150	°C
Storage temperature, T <sub>stg</sub>		-65	150	°C

- (1) Operation outside the Absolute Maximum Ratings may cause permanent device damage. Absolute Maximum Ratings do not imply functional operation of the device at these or any other conditions beyond those listed under Recommended Operating Conditions. If used outside the Recommended Operating Conditions but within the Absolute Maximum Ratings, the device may not be fully functional, and this may affect device reliability, functionality, performance, and shorten the device lifetime.

### 7.2 ESD Ratings

		VALUE	UNIT
V <sub>(ESD)</sub>	Electrostatic discharge	Human body model (HBM), per ANSI/ESDA/JEDEC JS-001 <sup>(1)</sup>	±2000
		Charged device model (CDM), per JEDEC specification JESD22-C101 <sup>(2)</sup>	±500

- (1) JEDEC document JEP155 states that 500-V HBM allows safe manufacturing with a standard ESD control process. Pins listed as ± 2000 V may actually have higher performance.  
(2) JEDEC document JEP157 states that 250-V CDM allows safe manufacturing with a standard ESD control process. Pins listed as ± 500 V may actually have higher performance.

### 7.3 Recommended Operating Conditions

over operating temperature range (unless otherwise noted)

		MIN	NOM	MAX	UNIT
V <sub>VM</sub>	Power supply voltage	VM	4.5	33	V
V <sub>VREF</sub>	Reference voltage	VREF	0	3.6	V
V <sub>IN</sub>	Logic input voltage	INx	0	5.5	V
f <sub>PWM</sub>	PWM frequency	INx	0	200	kHz
I <sub>OUT</sub> <sup>(1)</sup>	Peak output current	OUTx	0	3.7	A
I <sub>IPROPI</sub>	Peak output current	IPROPI	0	3	mA
T <sub>J</sub>	Operating junction temperature	-40	150	150	°C

- (1) Power dissipation and thermal limits must be observed

### 7.4 Thermal Information

THERMAL METRIC <sup>(1)</sup>		DRV8231A	DRV8231A	UNIT
		DDA (HSOP)	DSG (WSON)	
		8 PINS	8 PINS	
R <sub>θJA</sub>	Junction-to-ambient thermal resistance	42.8	66.5	°C/W
R <sub>θJC(top)</sub>	Junction-to-case (top) thermal resistance	57.6	77.8	°C/W
R <sub>θJB</sub>	Junction-to-board thermal resistance	16.8	32.8	°C/W

THERMAL METRIC <sup>(1)</sup>		DRV8231A	DRV8231A	UNIT
		DDA (HSOP)	DSG (WSON)	
		8 PINS	8 PINS	
$\Psi_{JT}$	Junction-to-top characterization parameter	5.4	2.2	°C/W
$\Psi_{JB}$	Junction-to-board characterization parameter	16.8	32.7	°C/W
$R_{\theta JC(bot)}$	Junction-to-case (bottom) thermal resistance	6.2	12.2	°C/W

(1) For more information about traditional and new thermal metrics, see the [Semiconductor and IC Package Thermal Metrics application report](#).

## 7.5 Electrical Characteristics

$4.5 \leq V_{VM} \leq 33$  V,  $-40^\circ C \leq T_J \leq 150^\circ C$  (unless otherwise noted). Typical values are at  $T_J = 25^\circ C$  and  $V_{VM} = 24$  V.

PARAMETER	TEST CONDITIONS	MIN	TYP	MAX	UNIT	
<b>POWER SUPPLY (VM)</b>						
$I_{VMQ}$	$V_{VM} = 24$ V, $IN1 = IN2 = 0$ , $T_J = 25^\circ C$			1	μA	
$I_{VM}$	$V_{VM} = 24$ V, $IN1 = IN2 = 1$		3	4	mA	
$t_{WAKE}$	Turnon time Control signal to active mode			250	μs	
$t_{SLEEP}$	Turnoff time Control signal to sleep mode	0.8	1.5	ms		
<b>LOGIC-LEVEL INPUTS (INx)</b>						
$V_{IL}$	Input logic low voltage		0.5		V	
$V_{IH}$	Input logic high voltage		1.5		V	
$V_{HYS}$	Input hysteresis		200		mV	
$I_{IL}$	Input logic low current $V_{IN} = 0$ V	-1	1	μA		
$I_{IH}$	Input logic high current $V_{IN} = 3.3$ V	33	100	μA		
$R_{PD}$	Input pulldown resistance To GND	100			kΩ	
<b>DRIVER OUTPUTS (OUTx)</b>						
$R_{DS(on)_HS}$	High-side MOSFET on resistance $V_{VM} = 24$ V, $I = 1$ A, $f_{PWM} = 25$ kHz	300			mΩ	
$R_{DS(on)_LS}$	Low-side MOSFET on resistance $V_{VM} = 24$ V, $I = 1$ A, $f_{PWM} = 25$ kHz	300			mΩ	
$V_{SD}$	Body diode forward voltage $I_{OUT} = 1$ A	0.8			V	
$t_{RISE}$	Output rise time $V_{VM} = 24$ V, OUTx rising from 10% to 90%	220			ns	
$t_{FALL}$	Output fall time $V_{VM} = 24$ V, OUTx falling from 90% to 10%	220			ns	
$t_{PD}$	Input to output propagation delay INx to OUTx	0.7	1	μs		
$t_{DEAD}$	Output dead time	200			ns	
<b>INTEGRATED CURRENT SENSE AND REGULATION (IPROPI, VREF)</b>						
$A_{IPROPI}$	Current mirror scaling factor	1500			μA/A	
$A_{ERR}$	Current mirror total error $I_{OUT} = 1$ A, $V_{VM} \geq 6.5$ V, $V_{IPROPI} \leq 3.0$ V	-6	6		%	
$t_{OFF}$	Current regulation off time	25			μs	
$t_{BLK}$	Current regulation blanking time	1.4			μs	
$t_{DELAY}$	Current sense delay time	1.1			μs	
$t_{DEG}$	Current regulation deglitch time	0.7			μs	
<b>PROTECTION CIRCUITS</b>						
$V_{UVLO}$	Supply undervoltage lockout (UVLO)	Supply rising	4.15	4.3	4.45	V
		Supply falling	4.05	4.2	4.35	V
$V_{UVLO\_HYS}$	Supply UVLO hysteresis	Rising to falling threshold	100			mV
$t_{UVLO}$	Supply undervoltage deglitch time		10			μs
$I_{OCP}$	Overcurrent protection trip point		3.7			A
$t_{OCP}$	Overcurrent protection deglitch time		1.5			μs
$t_{RETRY}$	Overcurrent protection retry time		3			ms

$4.5 \text{ V} \leq V_{VM} \leq 33 \text{ V}$ ,  $-40^\circ\text{C} \leq T_J \leq 150^\circ\text{C}$  (unless otherwise noted). Typical values are at  $T_J = 25^\circ\text{C}$  and  $V_{VM} = 24 \text{ V}$ .

PARAMETER	TEST CONDITIONS	MIN	TYP	MAX	UNIT
$T_{TSD}$	Thermal shutdown temperature		150	175	°C
$T_{HYS}$	Thermal shutdown hysteresis		40		°C

## 7.6 Typical Characteristics

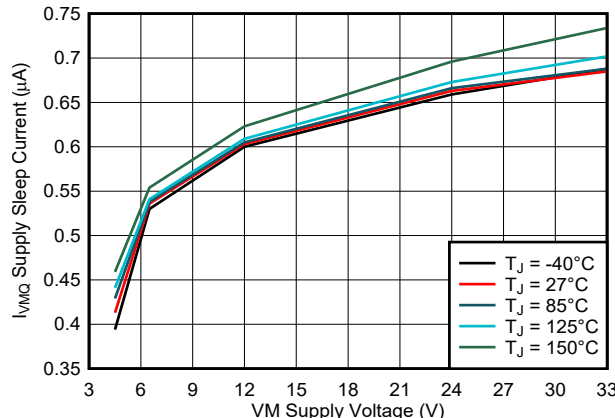


**Figure 7-1. Sleep Current ( $I_{VMQ}$ ) vs. Supply Voltage ( $V_{VM}$ )**

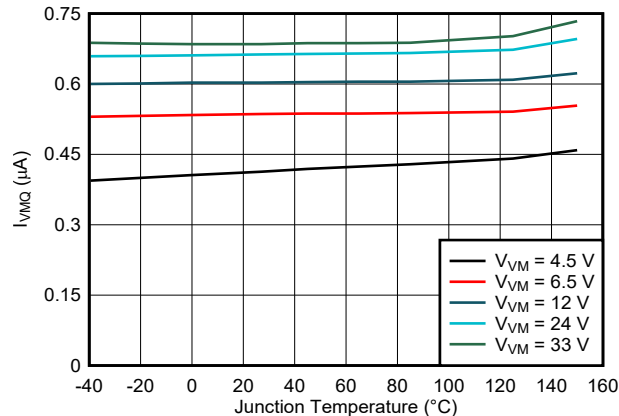


**Figure 7-2. Sleep Current ( $I_{VMQ}$ ) vs. Junction Temperature ( $T_J$ )**

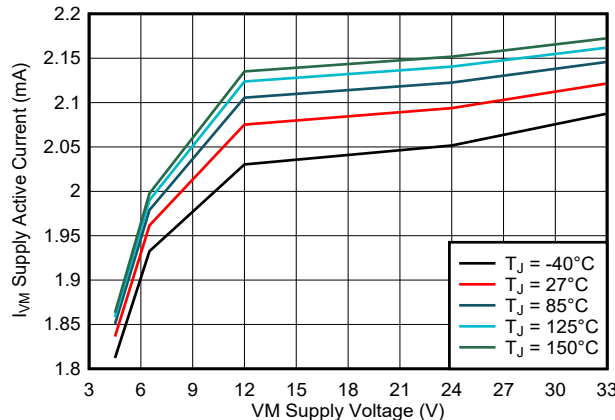


**Figure 7-3. Active Current ( $I_{VM}$ ) vs. Supply Voltage ( $V_{VM}$ )**

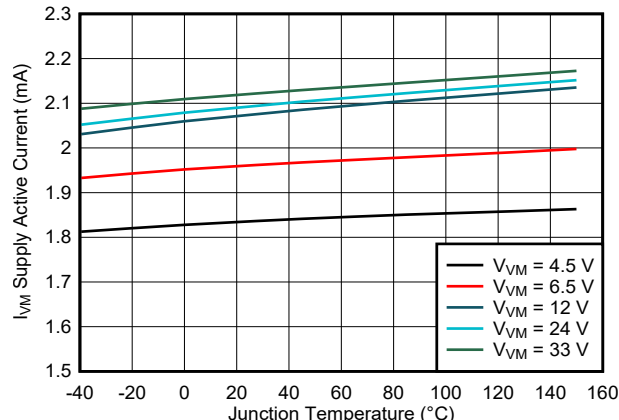


**Figure 7-4. Active Current ( $I_{VM}$ ) vs. Junction Temperature ( $T_J$ )**

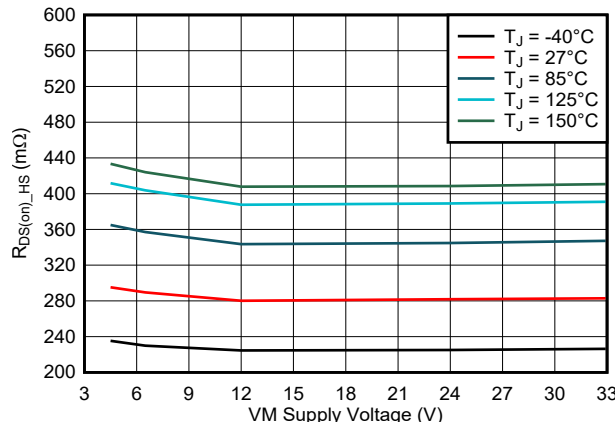


**Figure 7-5. High-Side R<sub>DS(on)</sub> vs. VM Supply Voltage**

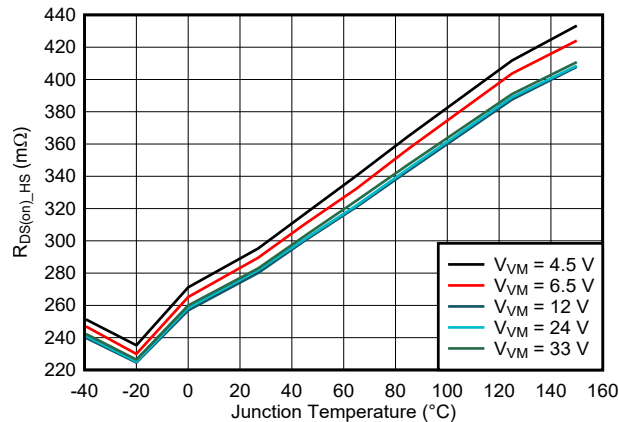


**Figure 7-6. High-Side R<sub>DS(on)</sub> vs. Junction Temperature (T<sub>J</sub>)**

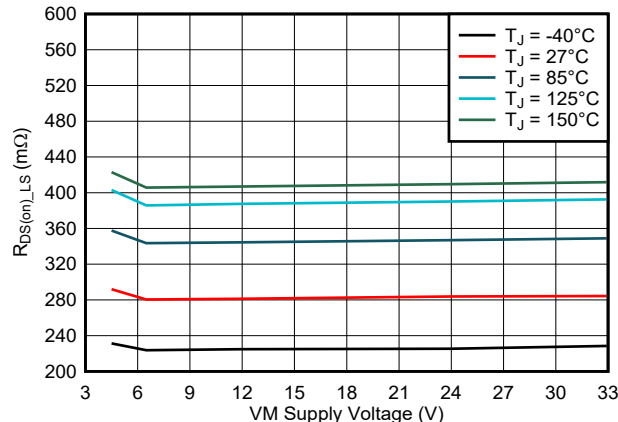


**Figure 7-7. Low-Side  $R_{DS(on)}$  vs. VM Supply Voltage**

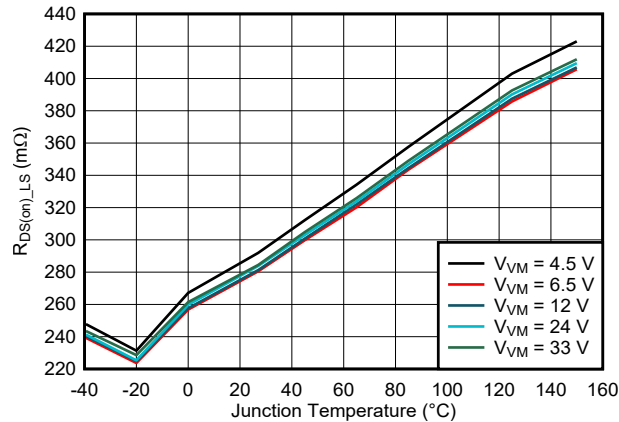


**Figure 7-8. Low-Side  $R_{DS(on)}$  vs. Junction Temperature ( $T_J$ )**

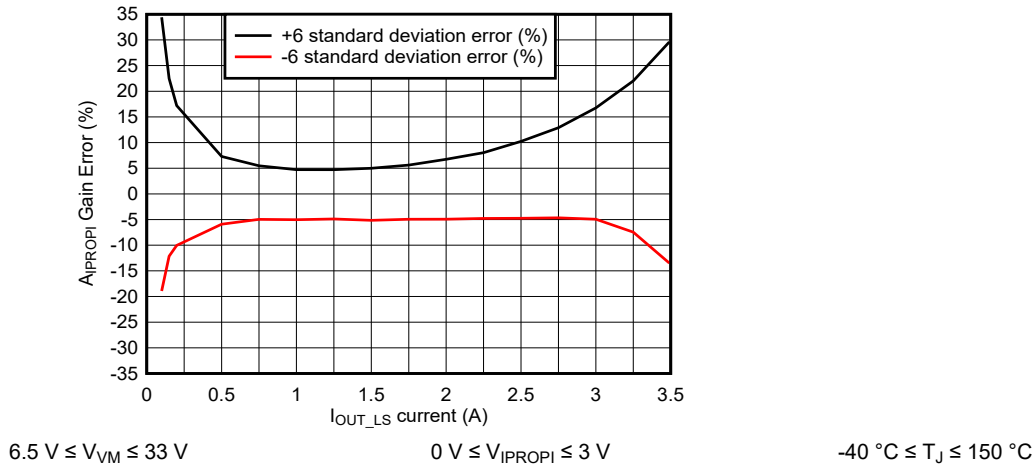


**Figure 7-9. Gain error of AIPROPI vs. Motor Current**

## 7.7 Timing Diagrams

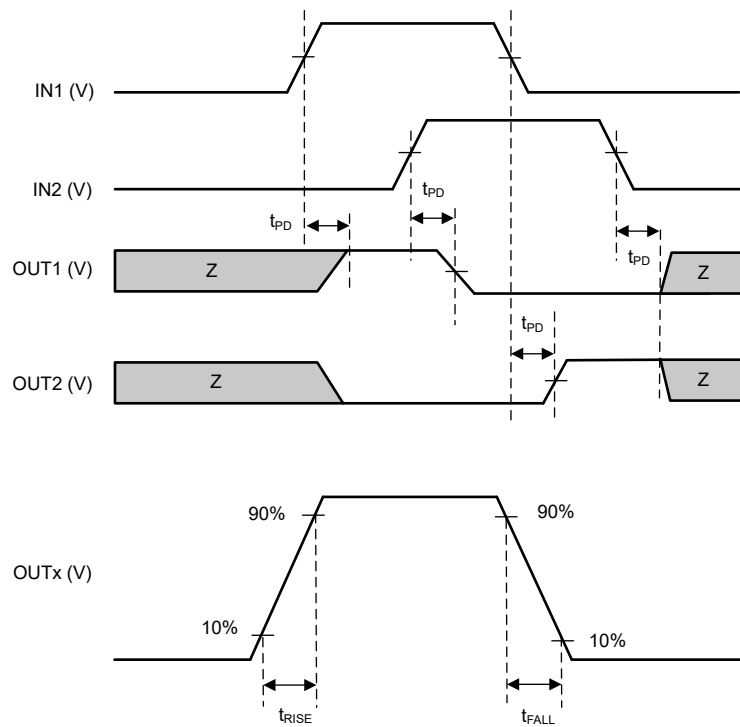


Figure 7-10. Input-to-Output Timing

## 8 Detailed Description

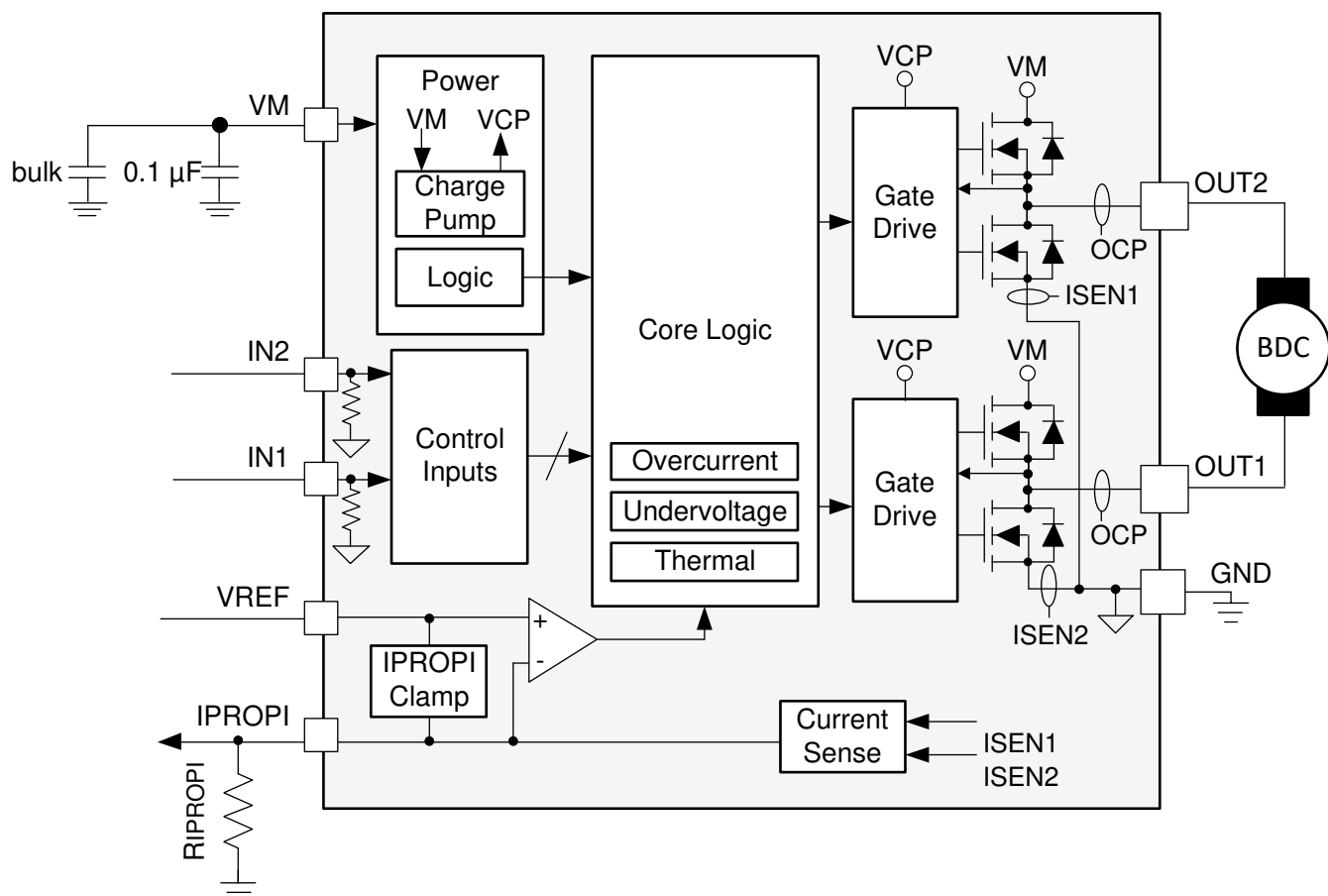
### 8.1 Overview

The DRV8231A is an 8-pin device for driving brushed DC motors from a 4.5-V to 33-V supply rail. Two logic inputs control the H-bridge driver, which consists of four N-channel MOSFETs that have a typical  $R_{DS(on)}$  of 600 mΩ (including one high-side and one low-side FET). A single power input, VM, serves as both device power and the motor winding bias voltage. The integrated charge pump of the device boosts VM internally and fully enhances the high-side FETs. Motor speed can be controlled with pulse-width modulation at frequencies between 0 to 200 kHz. The device enters a low-power sleep mode by bringing both inputs low.

The DRV8231A also integrates current sense feedback to a microcontroller using current mirrors on the low-side power MOSFETs. The IPROPI pin sources a small current that is proportional to the current in the MOSFETs. This current can be converted to a proportional voltage using an external resistor ( $R_{IPROPI}$ ). This integrated current sensing scheme out-performs traditional external shunt resistor sensing by providing current information even during the off-time slow decay recirculating period and removing the need for an external power shunt resistor. The integrated current regulation feature allows the device to limit the output current with a fixed off-time PWM chopping scheme. The VREF pin configures the current regulation level during motor operation to limit the load current.

A variety of integrated protection features protect the device in the case of a system fault. These include undervoltage lockout (UVLO), overcurrent protection (OCP), and overtemperature shutdown (TSD).

### 8.2 Functional Block Diagram



### 8.3 External Components

Table 8-1 lists the recommended external components for the device.

**Table 8-1. Recommended external components**

COMPONENT	PIN 1	PIN 2	RECOMMENDED
C <sub>VM1</sub>	VM	GND	0.1- $\mu$ F, low ESR ceramic capacitor, VM-rated.
C <sub>VM2</sub>	VM	GND	<a href="#">Section 10.1</a> , VM-rated.

## 8.4 Feature Description

### 8.4.1 Bridge Control

The DRV8231A output consists of four N-channel MOSFETs that are designed to drive high current. These outputs are controlled by the two logic inputs IN1 and IN2 as listed in [Table 8-2](#).

**Table 8-2. H-Bridge Control**

IN1	IN2	OUT1	OUT2	DESCRIPTION
0	0	High-Z	High-Z	Coast; H-bridge disabled to High-Z (sleep entered after 1 ms)
0	1	L	H	Reverse (Current OUT2 → OUT1)
1	0	H	L	Forward (Current OUT1 → OUT2)
1	1	L	L	Brake; low-side slow decay

The inputs can be set to static voltages for 100% duty cycle drive, or they can be pulse-width modulated (PWM) for variable motor speed. When using PWM, switching between driving and braking typically works best. For example, to drive a motor forward with 50% of the maximum RPM, IN1 = 1 and IN2 = 0 during the driving period, and IN1 = 1 and IN2 = 1 during the other period. Alternatively, the coast mode (IN1 = 0, IN2 = 0) for *fast current decay* is also available. [Figure 8-1](#) shows how the motor current flows through the H-bridge. The input pins can be powered before VM is applied.

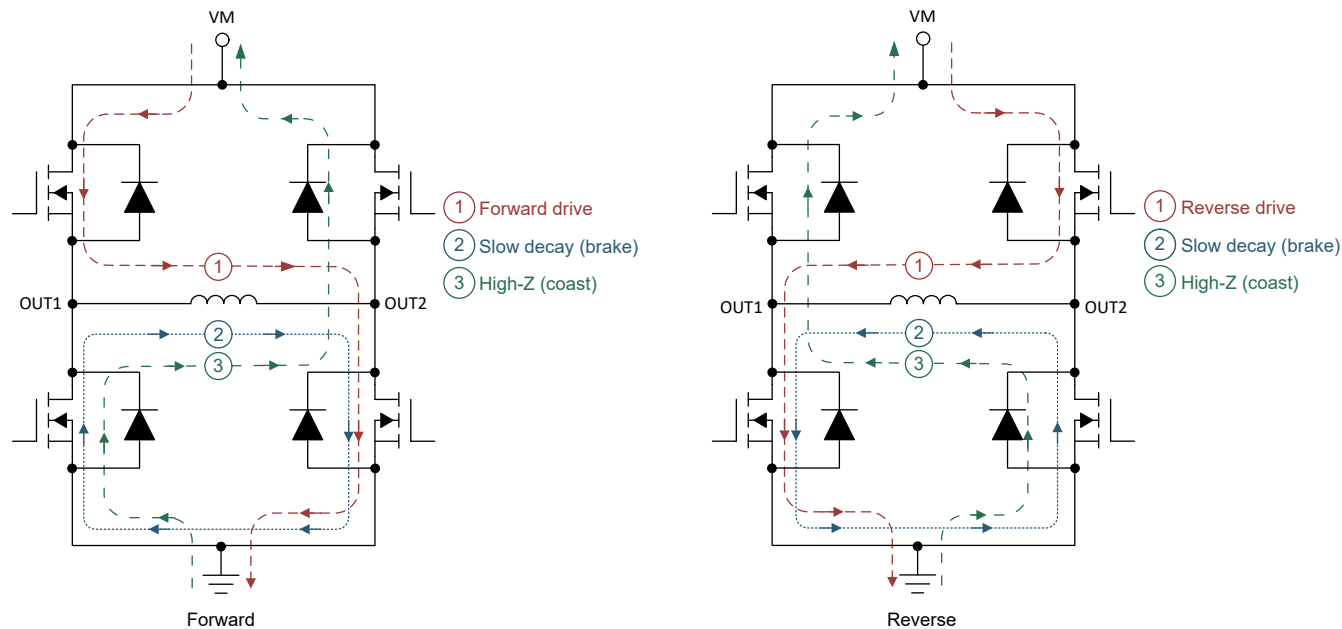


**Figure 8-1. H-Bridge Current Paths**

When an output changes from driving high to driving low, or driving low to driving high, dead time is automatically inserted to prevent shoot-through. The  $t_{DEAD}$  time is the time in the middle when the output is High-Z. If the output pin is measured during  $t_{DEAD}$ , the voltage depends on the direction of current. If the current is leaving the pin, the voltage is a diode drop below ground. If the current is entering the pin, the voltage is a diode drop above VM. This diode is the body diode of the high-side or low-side FET.

The propagation delay time ( $t_{PD}$ ) is measured as the time between an input edge to output change. This time accounts for input deglitch time and other internal logic propagation delays. The input deglitch time prevents noise on the input pins from affecting the output state. Additional output slew delay timing accounts for FET turn on or turn off times ( $t_{RISE}$  and  $t_{FALL}$ ).

[Figure 8-2](#) below shows the timing of the inputs and outputs of the motor driver.

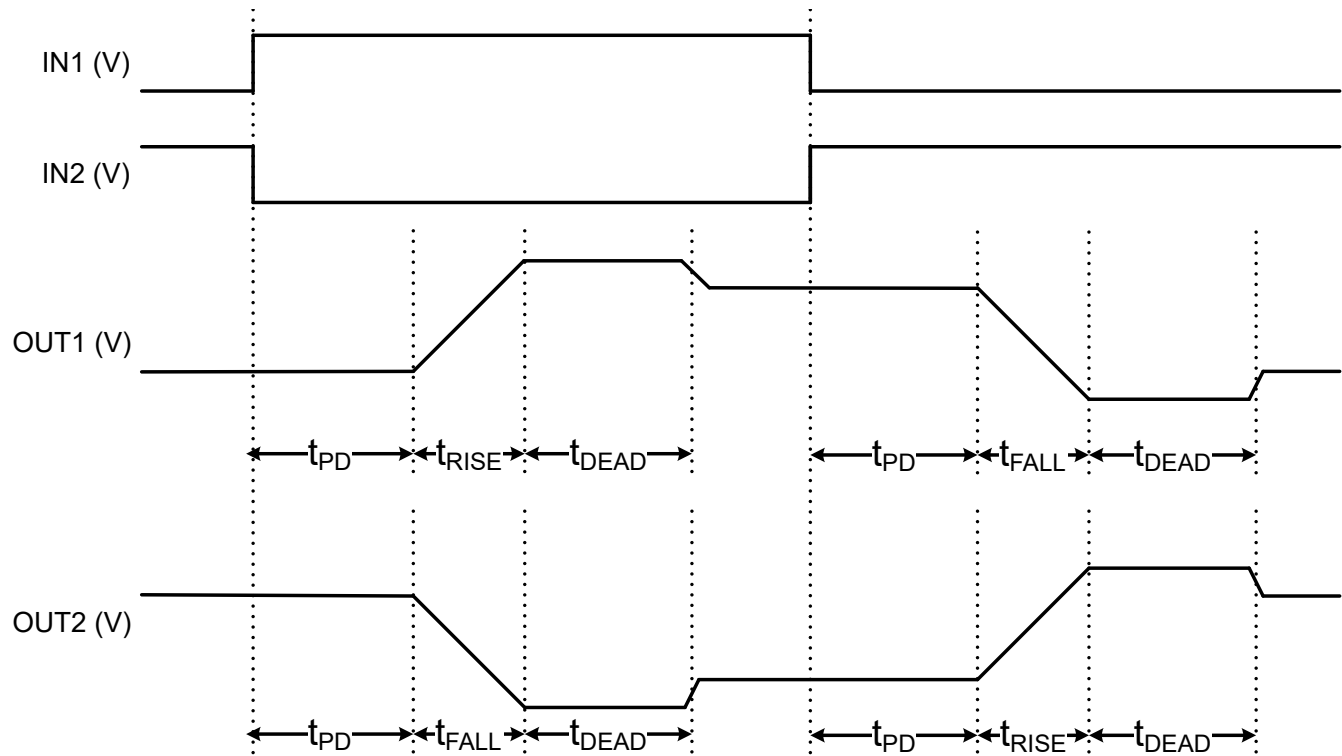
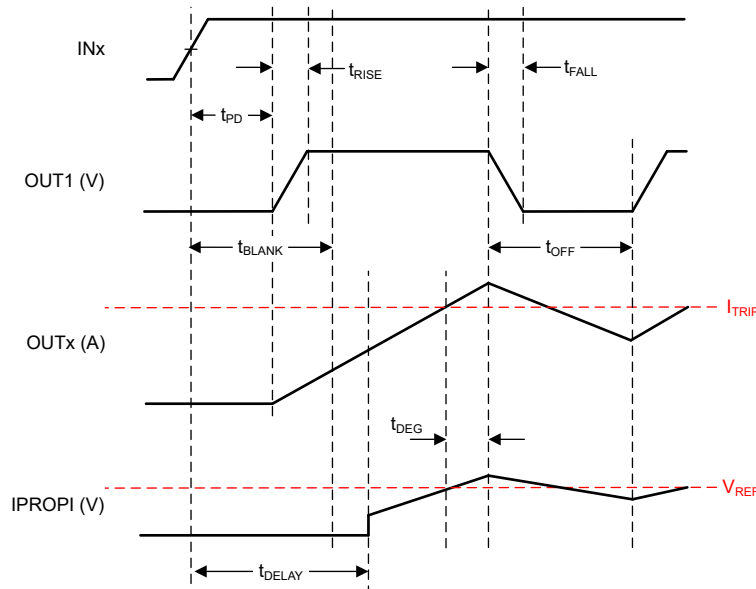


Figure 8-2. H-Bridge Current Paths

### 8.4.2 Current Sense and Regulation (IPROPI)

The DRV8231A device integrates current sensing, regulation, and feedback as part of the IPROPI feature. These features allow the device to sense the output current without an external sense resistor or sense circuitry reducing system size, cost, and complexity. This also allows for the device to limit the output current in the case of motor stall or high torque events and give detailed feedback to the controller about the load current through a current proportional output. [Figure 8-3](#) shows the IPROPI timings specified in the Electrical Characteristics table.



**Figure 8-3. Detailed IPROPI Timing Diagram**

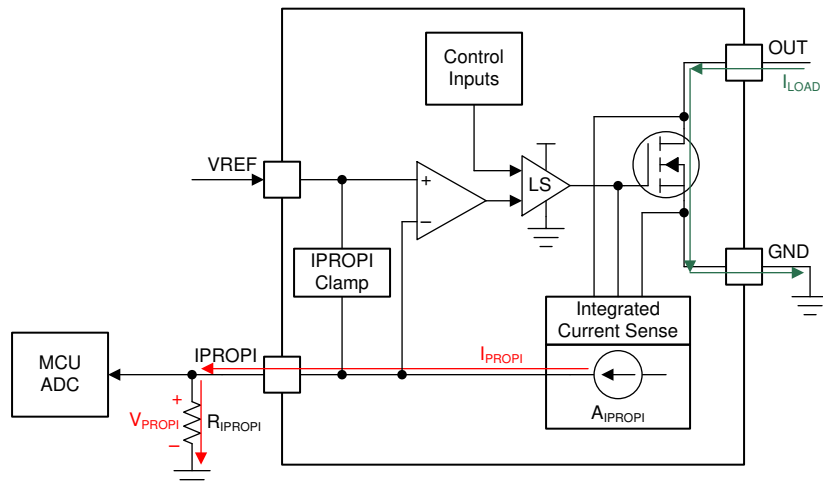
#### 8.4.2.1 Current Sensing

The IPROPI pin outputs an analog current proportional to the current flowing through the low-side power MOSFETs in the H-bridge scaled by  $A_{IPROPI}$ . The IPROPI output current can be calculated by [Equation 1](#). The  $I_{LSx}$  in [Equation 1](#) is only valid when the current flows from drain to source in the low-side MOSFET. If current flows from source to drain or through the body diode, the value of  $I_{LSx}$  for that channel is zero. For instance, if the bridge is in the brake, slow-decay state, then the current out of IPROPI is only proportional to the current in one of the low-side MOSFETs.

$$I_{IPROPI} (\mu\text{A}) = (I_{LS1} + I_{LS2}) (\text{A}) \times A_{IPROPI} (\mu\text{A}/\text{A}) \quad (1)$$

The  $A_{ERR}$  parameter in the Electrical Characteristics table is the error associated with the  $A_{IPROPI}$  gain. It indicates the combined effect of offset error added to the  $I_{OUT}$  current and gain error.

The motor current is measured by an internal current mirror architecture on the low-side FETs which removes the need for an external power sense resistor as shown in [Figure 8-4](#). The current mirror architecture allows for the motor winding current to be sensed in both the drive and brake low-side slow-decay periods allowing for continuous current monitoring in typical bidirectional brushed DC motor applications. In coast mode, the current is freewheeling and cannot be sensed because it flows from source to drain. However, the current can be sampled by briefly reenabling the driver in either drive or slow-decay modes and measuring the current before switching back to coast mode again.



Copyright © 2017, Texas Instruments Incorporated

**Figure 8-4. Integrated Current Sensing**

The IPROPI pin should be connected to an external resistor ( $R_{IPROPI}$ ) to ground in order to generate a proportional voltage ( $V_{IPROPI}$ ) on the IPROPI pin with the  $I_{IPROPI}$  analog current output. This allows for the load current to be measured as the voltage drop across the  $R_{IPROPI}$  resistor with a standard analog to digital converter (ADC). The  $R_{IPROPI}$  resistor can be sized based on the expected load current in the application so that the full range of the controller ADC is utilized. Additionally, the DRV8251A device implements an internal IPROPI voltage clamp circuit to limit  $V_{IPROPI}$  with respect to  $V_{VREF}$  on the VREF pin and protect the external ADC in case of output overcurrent or unexpected high current events.

The corresponding IPROPI voltage to the output current can be calculated by [Equation 2](#).

$$V_{IPROPI} (V) = I_{IPROPI} (A) \times R_{IPROPI} (\Omega) \quad (2)$$

The IPROPI output bandwidth is limited by the sense delay time ( $t_{DELAY}$ ) of the internal current sensing circuit. This time is the delay from the low-side MOSFET enable command (from the INx pins) to the IPROPI output being ready.

If the device is alternating between drive and slow-decay (brake) in an H-bridge PWM pattern then the low-side MOSFET sensing the current is continuously on and the sense delay time has no impact to the IPROPI output. If a command on the INx pins disables the low-side MOSFETs (according to the logic tables in [Section 8.4.1](#)), the IPROPI output will disable with the input logic signal. Although the low-side MOSFETs may still conduct current as they disable according to the device slew rate (noted in the Electrical Characteristics table by  $t_{RISE}$  time), IPROPI will not represent the current in the low-side MOSFETs during this turnoff time.

#### 8.4.2.2 Current Regulation

The DRV8231A device integrates current regulation using a fixed off-time current chopping scheme. This allows the devices to limit the output current in case of motor stall, high torque, or other high current load events without involvement from the external controller as shown in [Figure 8-5](#).

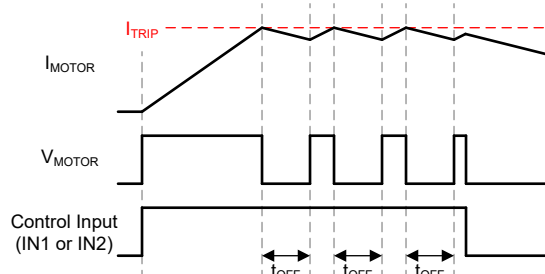


**Figure 8-5. Off-Time Current-Regulation**

The current chopping threshold ( $I_{TRIP}$ ) is set through a combination of the VREF voltage ( $V_{VREF}$ ) and IPROPI output resistor ( $R_{IPROPI}$ ). This is done by comparing the voltage drop across the external  $R_{IPROPI}$  resistor to  $V_{VREF}$  with an internal comparator.

$$I_{TRIP} (\text{A}) \times A_{IPROPI} (\mu\text{A}/\text{A}) = V_{VREF} (\text{V}) / R_{IPROPI} (\Omega) \quad (3)$$

For example, if  $V_{VREF} = 3.3 \text{ V}$ ,  $R_{IPROPI} = 1375 \Omega$ , and  $A_{IPROPI} = 1500 \mu\text{A}/\text{A}$ , then  $I_{TRIP}$  will be approximately 1.6 A.

The fixed off-time current chopping scheme supports up to 100% duty cycle current regulation since the H-bridge automatically enables after the  $t_{OFF}$  period and does not require a new control input edge on the INx pins to reset the outputs. When the motor current exceeds the  $I_{TRIP}$  threshold, the outputs will enter a current chopping mode with a fixed off time ( $t_{OFF}$ ). During  $t_{OFF}$ , the H-bridge enters a brake/low-side slow decay state (both low-side MOSFETs ON) for  $t_{OFF}$  duration after  $I_{OUT}$  exceeds  $I_{TRIP}$ . After  $t_{OFF}$ , the outputs re-enable according to the control inputs if  $I_{OUT}$  is less than  $I_{TRIP}$ . If  $I_{OUT}$  is still greater than  $I_{TRIP}$ , the H-bridge enters another period of brake/low-side slow decay for  $t_{OFF}$ . If the state of the INx control pins changes during the  $t_{OFF}$  time, the remainder of the  $t_{OFF}$  time is ignored, and the outputs will again follow the inputs.

The  $I_{TRIP}$  comparator has both a blanking time ( $t_{BLK}$ ) and a deglitch time ( $t_{DEG}$ ). The internal blanking time helps to prevent voltage and current transients during output switching from effecting the current regulation. These transients may be caused by a capacitor inside the motor or on the connections to the motor terminals. The internal deglitch time ensures that transient conditions do not prematurely trigger the current regulation. In certain cases where the transient conditions are longer than the deglitch time, placing a 10-nF capacitor on the IPROPI pin, close to the device, will help filter the transients on IPROPI output so current regulation does not prematurely trigger. The capacitor value can be adjusted as needed, however large capacitor values may slow down the response time of the current regulation circuitry.

The internal current regulation and current feedback can be disabled by tying IPROPI to GND and setting the VREF pin voltage greater than GND. If current feedback is required and current regulation is not required, set  $V_{VREF}$  and  $R_{IPROPI}$  such that  $V_{IPROPI}$  never reaches the  $V_{VREF}$  threshold. For proper operation of the current regulation circuit,  $V_{VREF}$  must be within the range of the VREF pin voltages specified in the Recommended Operating Conditions table.

### 8.4.3 Protection Circuits

The DRV8231A device is fully protected against VM undervoltage, overcurrent, and overtemperature events.

#### 8.4.3.1 Overcurrent Protection (OCP)

An analog current limit circuit on each FET limits the current through the FET by limiting the gate drive internally. If this analog current limit persists for longer than the OCP deglitch time ( $t_{OCP}$ ), all FETs in the H-bridge will disable. The driver re-enables after the OCP retry period ( $t_{RETRY}$ ) has passed. If the fault condition is still present, the cycle repeats as shown in Figure 8-6.

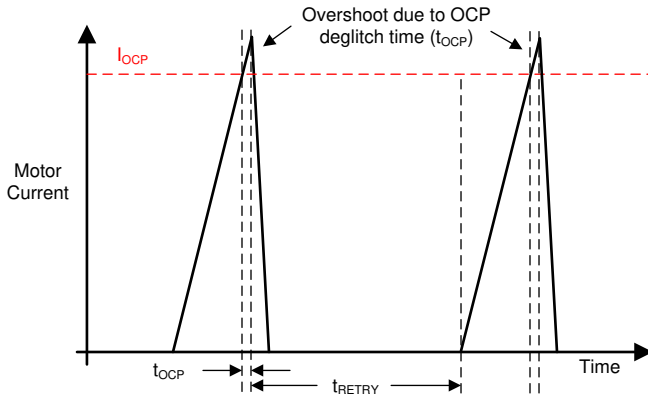


**Figure 8-6. OCP Operation**

Overcurrent conditions are detected independently on both high- and low-side FETs. This means that a short to ground, supply, or across the motor winding will all result in an overcurrent shutdown. Overcurrent protection does not use the current sense circuitry used for current regulation, so it functions regardless of VREF and IPROPI settings.

#### 8.4.3.2 Thermal Shutdown (TSD)

If the die temperature exceeds safe limits, all FETs in the H-bridge are disabled. After the die temperature has fallen to a safe level, operation automatically resumes.

#### 8.4.3.3 VM Undervoltage Lockout (UVLO)

Whenever the voltage on the VM pin falls below the UVLO falling threshold voltage,  $V_{UVLO}$ , all circuitry in the device is disabled, the output FETs are disabled, and all internal logic is reset. Operation continues when the  $V_{VM}$  voltage rises above the UVLO rising threshold as shown in Figure 8-7.

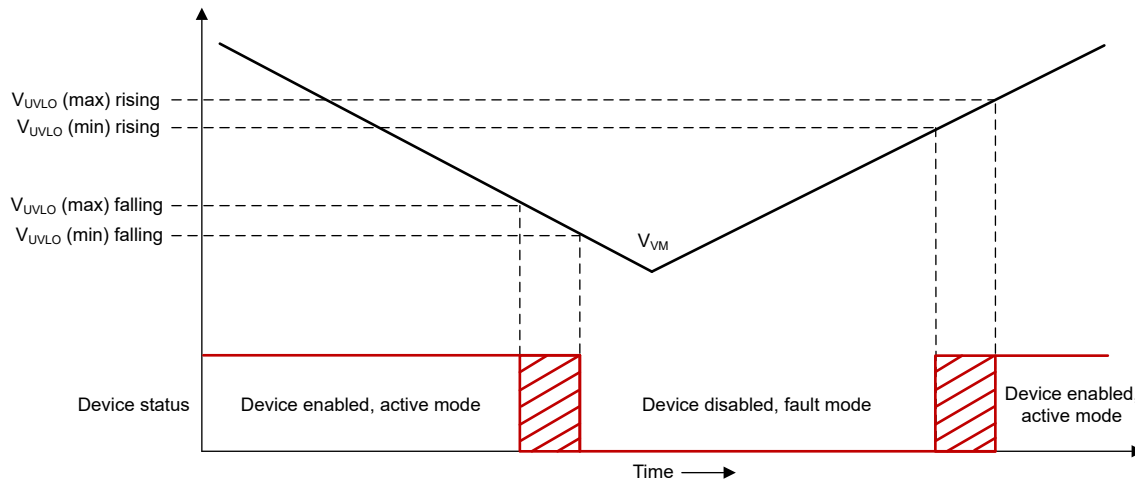


**Figure 8-7. VM UVLO Operation**

## 8.5 Device Functional Modes

Table 8-3 summarizes the DRV8231A functional modes described in this section.

**Table 8-3. Modes of Operation**

MODE	CONDITION	H-BRIDGE	INTERNAL CIRCUITS
Active Mode	IN1 or IN2 = logic high	Operating	Operating
Low-Power Sleep Mode	IN1 = IN2 = logic low	Disabled	Disabled
Fault Mode	Any fault condition met	Disabled	See Table 8-4

### 8.5.1 Active Mode

After the supply voltage on the VM pin has crossed the undervoltage threshold  $V_{UVLO}$ , the INx pins are in a state other than  $IN1 = 0$  &  $IN2 = 0$ , and  $t_{WAKE}$  has elapsed, the device enters active mode. In this mode, the H-bridge, charge pump, and internal logic are active and the device is ready to receive inputs.

### 8.5.2 Low-Power Sleep Mode

When the IN1 and IN2 pins are both low for time  $t_{SLEEP}$ , the DRV8231A device enters a low-power sleep mode. In sleep mode, the outputs remain High-Z and the device draws minimal current from the supply pin ( $I_{VMQ}$ ). If the device is powered up while all inputs are low, it immediately enters sleep mode. After any of the input pins are set high for longer than the duration of  $t_{WAKE}$ , the device becomes fully operational. Figure 8-8 shows an example timing diagram for entering and leaving sleep mode.

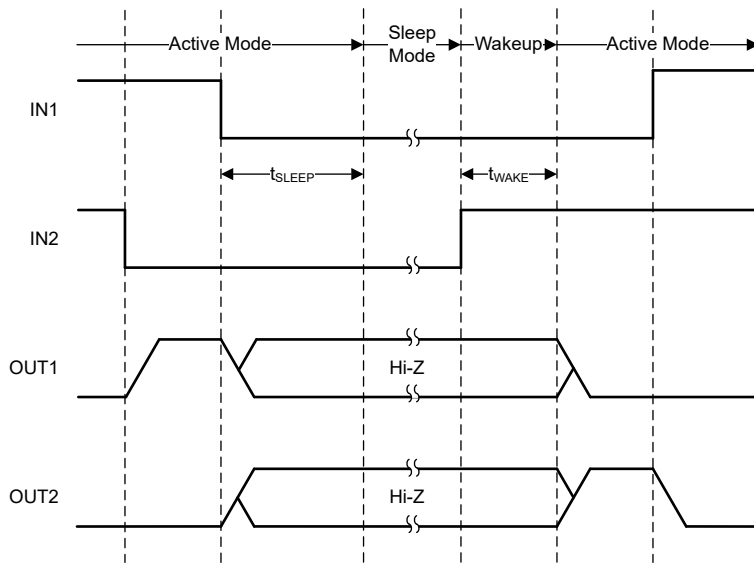


**Figure 8-8. Sleep Mode Entry and Wakeup Timing Diagram**

### 8.5.3 Fault Mode

The DRV8231A device enters a fault mode when a fault is encountered. This is utilized to protect the device and the output load. The device behavior in the fault mode is described in Table 8-4 and depends on the fault condition. The device will leave the fault mode and re-enter the active mode when the recovery condition is met.

**Table 8-4. Fault Conditions Summary**

FAULT	CONDITION	H-BRIDGE	INTERNAL CIRCUITS	RECOVERY
VM undervoltage (UVLO)	$V_M < V_{UVLO,falling}$	Disabled	Disabled	$V_M > V_{UVLO,rising}$
Overcurrent (OCP)	$I_{OUT} > I_{OCP}$	Disabled	Operating	$I_{OUT} < I_{OCP}$
Thermal Shutdown (TSD)	$T_J > T_{TSD}$	Disabled	Operating	$T_J < T_{TSD} - T_{HYS}$

## 8.6 Pin Diagrams

### 8.6.1 Logic-Level Inputs

Figure 8-9 shows the input structure for the logic-level input pins IN1, IN2, PH/IN1, and EN/IN2.

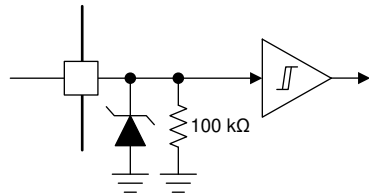


**Figure 8-9. Logic-level input**

## 9 Application and Implementation

### Note

Information in the following applications sections is not part of the TI component specification, and TI does not warrant its accuracy or completeness. TI's customers are responsible for determining suitability of components for their purposes. Customers should validate and test their design implementation to confirm system functionality.

### 9.1 Application Information

The DRV8231A device is typically used to drive one brushed DC motor.

### 9.2 Typical Application

#### 9.2.1 Brush DC Motor

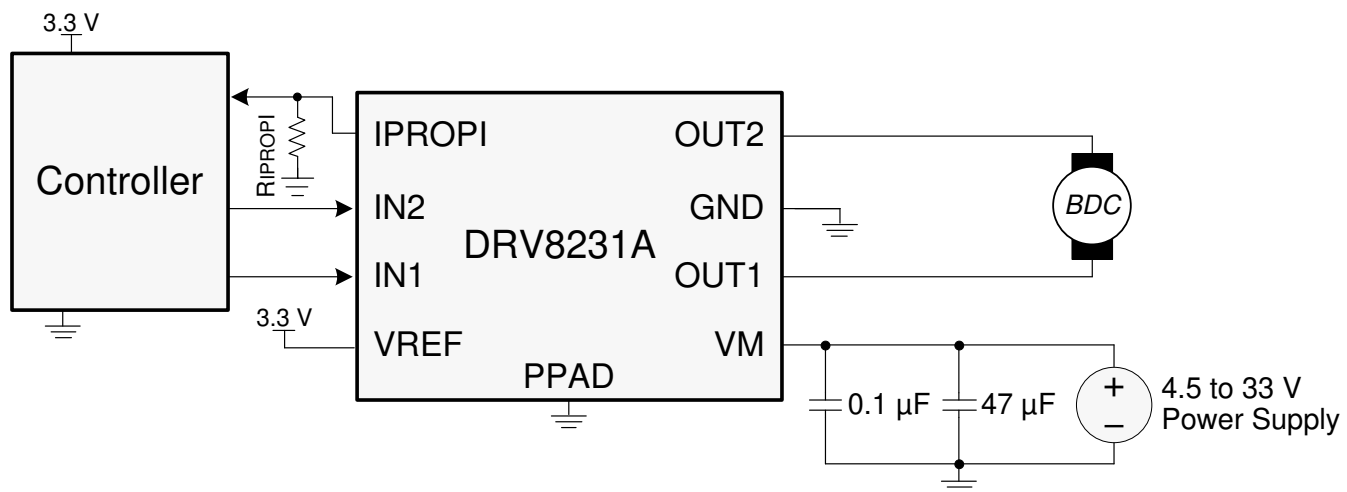


Figure 9-1. Typical Connections

#### 9.2.1.1 Design Requirements

The table below lists the design parameters.

Table 9-1. Design Parameters

DESIGN PARAMETER	REFERENCE	EXAMPLE VALUE
Motor voltage	$V_{VM}$	12 V
Average motor current	$I_{AVG}$	0.8 A
Motor inrush (startup) current	$I_{INRUSH}$	2.1 A
Motor stall current	$I_{STALL}$	2.1 A
Motor current trip point	$I_{TRIP}$	1.9 A
VREF voltage	VREF	3.3 V
IPROPI sense resistance	$R_{IPROPI}$	1.5 kΩ
PWM frequency	$f_{PWM}$	50 kHz

#### 9.2.1.2 Detailed Design Procedure

##### 9.2.1.2.1 Motor Voltage

The motor voltage to use depends on the ratings of the motor selected and the desired RPM. A higher voltage spins a brushed DC motor faster with the same PWM duty cycle applied to the power FETs. A higher voltage also increases the rate of current change through the inductive motor windings.

### 9.2.1.2.2 Motor Current

Motors experience large currents at low speed, initial startup, and stalled rotor conditions. The large current at motor startup is sometimes called inrush current. The current regulation feature in the DRV8231A can help to limit these large currents. Figure 9-4 and Figure 9-5 show examples of limiting inrush current.

Alternatively, the microcontroller may limit the inrush current by ramping the PWM duty cycle during the startup time.

### 9.2.1.3 Application Curves

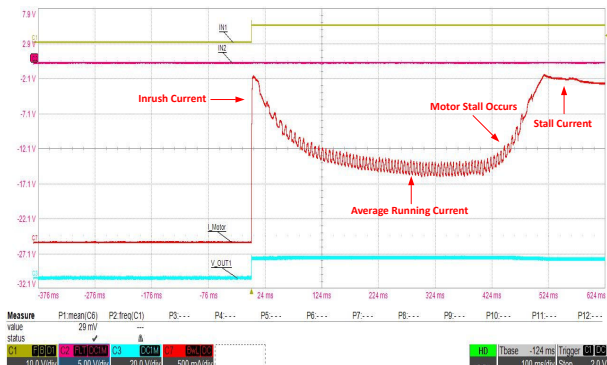


**Figure 9-2. Motor startup at 100% duty cycle**

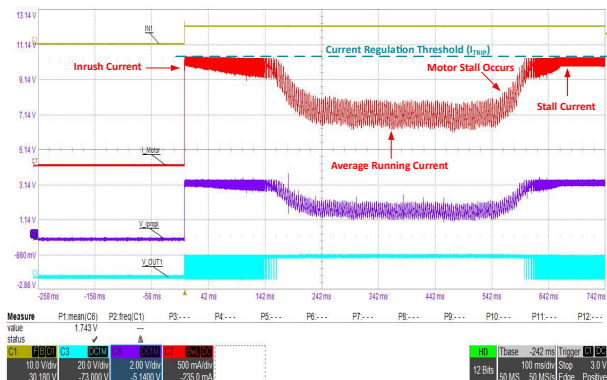


**Figure 9-4. Motor startup at 100% duty cycle with current regulation**

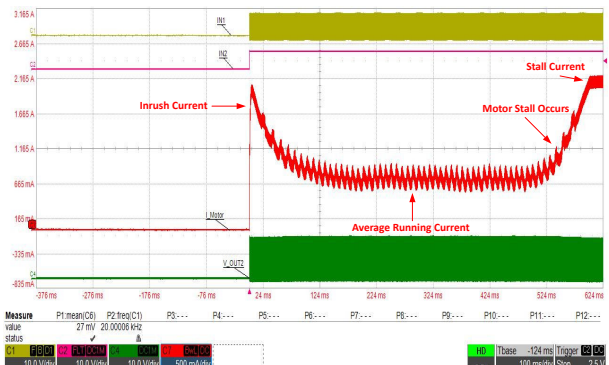


**Figure 9-3. Motor startup at 50% duty cycle**

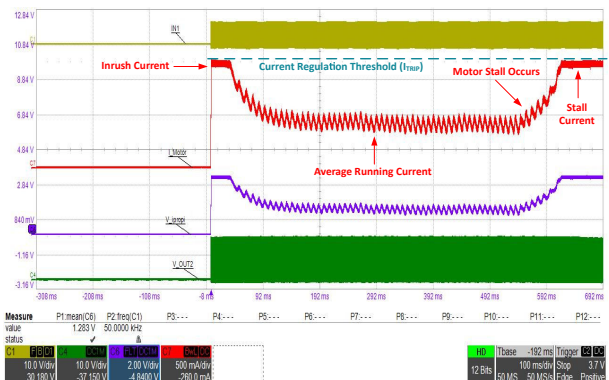


**Figure 9-5. Motor startup at 50% duty cycle with current regulation**

### 9.2.2 Stall Detection

Some applications require stall detection to notify the microcontroller of a locked rotor condition. A stall could be caused by one of two things: unintended mechanical blockage or the load reaching an end-stop in a constrained travel path. By using the IPROPI analog current sense feedback of the DRV8231A, the system can implement a simple stall detection scheme.

The principle of this stall detection scheme relies on the fact that motor current increases during stall conditions as shown in Figure 9-6. To implement stall detection, the microcontroller reads the voltage on the IPROPI pin using an ADC and compares it to a stall threshold set in firmware. Alternatively, a comparator peripheral may be used to set this threshold as well.

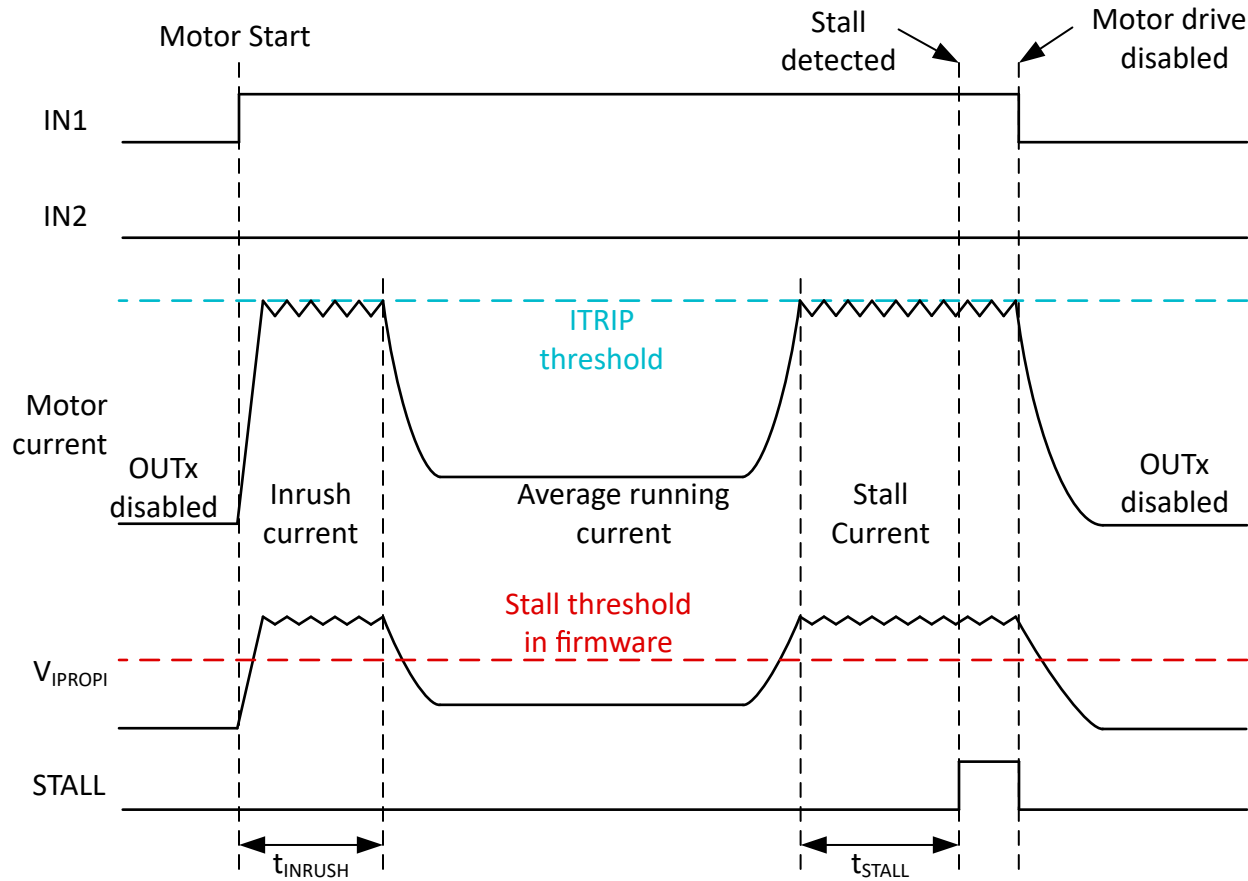


**Figure 9-6. Motor Current Profile with STALL Signal**

### 9.2.2.1 Design Requirements

The table below lists the design parameters.

**Table 9-2. Design Parameters**

DESIGN PARAMETER	REFERENCE	EXAMPLE VALUE
Motor voltage	$V_M$	14.4 V
Motor current trip point	$I_{TRIP}$	900 mA
VREF voltage	VREF	2 V
IPROPI resistance	$R_{IPROPI}$	1.5 kΩ
Stall current trip point	$I_{STALL}$	500 mA
Stall IPROPI voltage trip point	$V_{IPROPI,STALL}$	1 V
Inrush current ignore time	$t_{INRUSH}$	65 ms
Stall detection time	$t_{STALL}$	65 ms

### 9.2.2.2 Detailed Design Procedure

#### 9.2.2.2.1 Stall Detection Timing

The microcontroller needs to decide whether or not the IPROPI signal indicates a motor stall. Large inrush current occurs during motor start up because motor speed is low. As the motor accelerates, the motor current drops to an average level because the back electromotive force (EMF) in the motor increases with speed. The inrush current should not be mistaken for a stall condition. One way to do this is for the microcontroller to ignore the IPROPI signal above the firmware stall threshold for the duration of the inrush current,  $t_{INRUSH}$ , at startup. The  $t_{INRUSH}$  timing should be determined experimentally because it depends on motor parameters, supply voltage, and mechanical load response times.

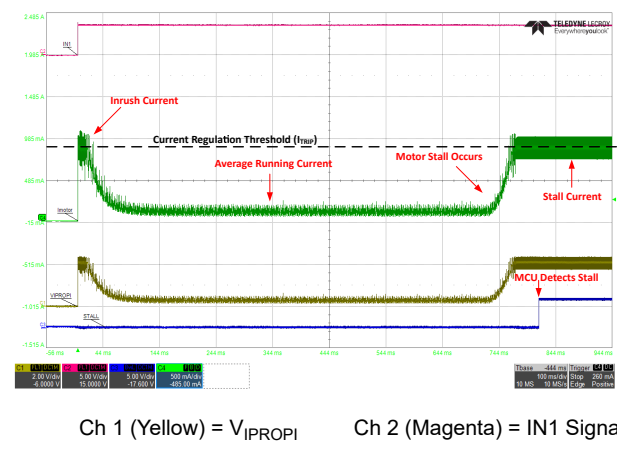
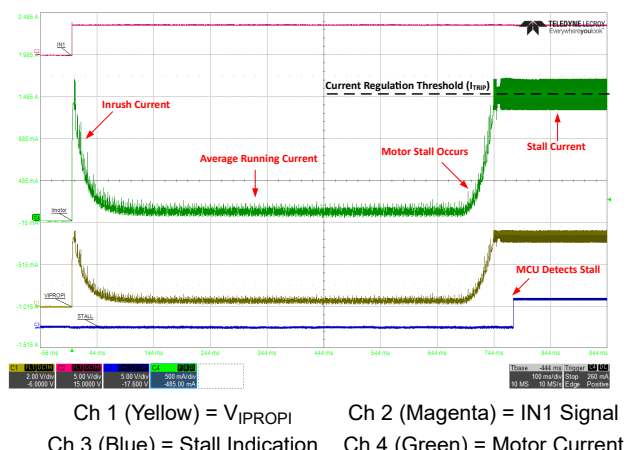
When a stall condition occurs, the motor current will increase from the average running current level because the back EMF is now 0 V. In some cases, it may be desirable to drive at the stall current for some time in case the motor can clear the blockage on its own. This might be useful for an unintended stall or high-torque condition on the motor. In this case, the system designer can choose a long stall detection time,  $t_{STALL}$ , before the microcontroller decides to take action. In other cases, like end-stop detection, a faster response might be desired to reduce power or minimize strong motor torque on the gears or end-stop. This corresponds to setting a shorter  $t_{STALL}$  time in the microcontroller.

Figure 9-6 illustrates the  $t_{INRUSH}$  and  $t_{STALL}$  timings and how they relate to the motor current waveform.

### 9.2.2.2 Stall Threshold Selection

The stall detection threshold in firmware should be chosen at a current level between the maximum stall current and the average running current of the motor as shown in Figure 9-6.

### 9.2.2.3 Application Curves



**Figure 9-7. Example Waveform of Stall Detection**

**Figure 9-8. Stall Detected on IPROPI While Current Regulation Limits Inrush and Stall Currents**

### 9.2.3 Relay Driving

The PWM interface may also be used to drive single- and dual-coil latching relays, as shown in the figures below.

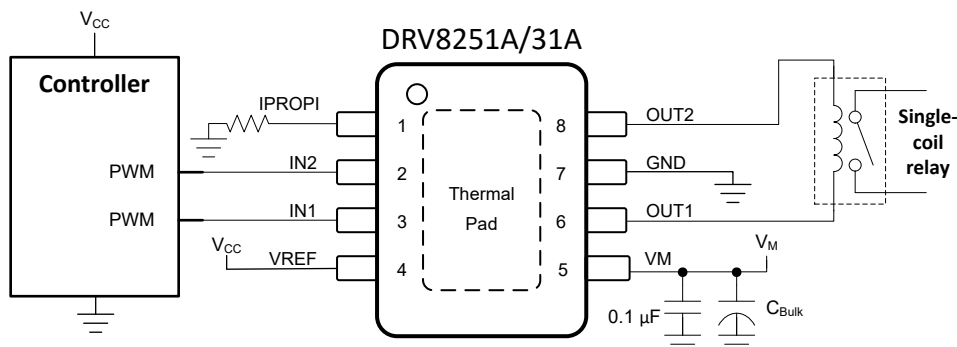


**Figure 9-9. Single-Coil Relay Driving**

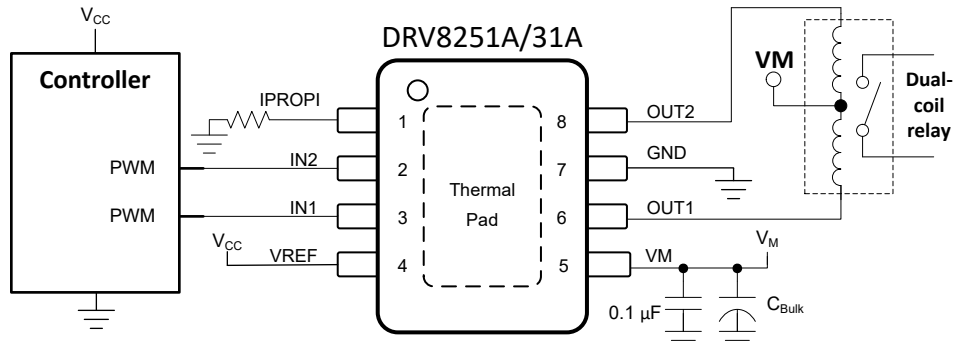


**Figure 9-10. Dual-Coil Relay Driving**

### 9.2.3.1 Design Requirements

Table 9-3 provides example requirements for a single- or dual-coil relay application. Current regulation may also be configured to ensure the relay current is within the relay specification. This is important if the VM supply voltage is higher than the voltage rating of the relay.

**Table 9-3. System design requirements**

DESIGN PARAMETER	REFERENCE	EXAMPLE VALUE
Motor supply voltage	V <sub>M</sub>	12 V
Microcontroller supply voltage	V <sub>CC</sub>	3.3 V
Single coil relay current	I <sub>Relay</sub>	500 mA pulse for 200 ms
Dual coil relay current	I <sub>OUT1</sub> , I <sub>OUT2</sub>	100 mA pulse for 200 ms

### 9.2.3.2 Detailed Design Procedure

#### 9.2.3.2.1 Control Interface for Single-Coil Relays

The PWM interface can be used to drive single-coil relays. To actuate the relay, the driver needs to drive current with either the forward or reverse states in the PWM table. After driving the relay, the outputs can be disabled (IN1=IN2=0) to put the driver to sleep and save energy. Alternatively, the outputs can be put into brake mode briefly after actuation to avoid back EMF effects from the relay or causing current to flow back from the relay into the VM supply node.

#### 9.2.3.2.2 Control Interface for Dual-Coil Relays

A dual coil relay only require two low-side drivers if the center tap is connected to VM. The body diodes of the unused FETs act as freewheeling diodes, so additional freewheeling diodes are not needed when driving a dual-coil relay with the DRV8231A. The PWM interface can be used to control the dual-coil relay. The following figures show the schematic and timing diagram for driving dual-coil relays.

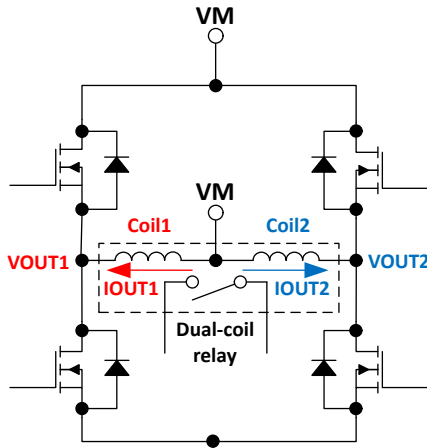


Figure 9-11. Schematic of dual-coil relay driven by the OUTx H-bridge

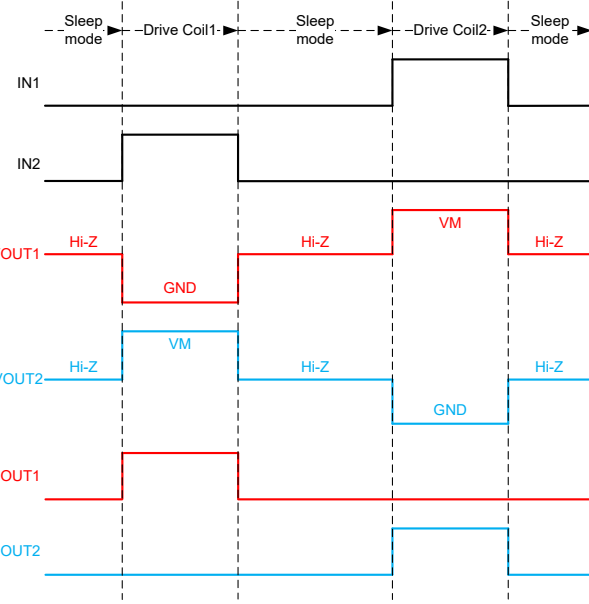


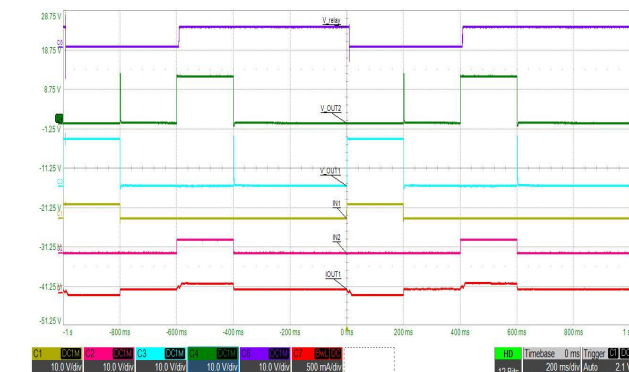
Figure 9-12. Timing diagram for driving a dual-coil relay with PWM interface

Table 9-4 shows the logic table for the PWM interface. The descriptions in this table reflect how the input and output states drive the dual coil relay. When Coil1 is driven (OUT1 voltage is at GND), The voltage at OUT2 will go to VM. Because the center tap of the relay is also at VM, no current flows through Coil2. The same is true when Coil2 is driven; Coil1 shorts to VM. The body diodes of the high-side FETs act as freewheeling diodes, so extra external diodes are not needed. Figure 9-15 shows oscilloscope traces for this application.

Table 9-4. PWM control table for dual-coil relay driving

IN1	IN2	OUT1	OUT2	DESCRIPTION
0	0	Hi-Z	Hi-Z	Outputs disabled (H-Bridge Hi-Z)
0	1	L	H	Drive Coil1
1	0	H	L	Drive Coil2
1	1	L	L	Drive Coil1 and Coil2 (invalid state for a dual-coil latching relay)

### 9.2.3.3 Application Curves



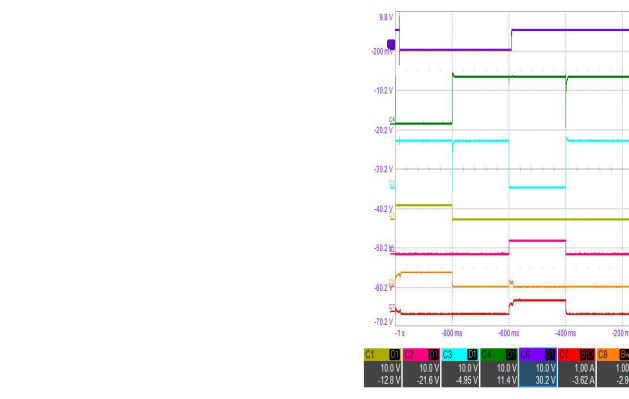
A. Ch 1 = IN1      Ch 2 = IN2      Ch 3 = V<sub>OUT1</sub>  
Ch 4 = V<sub>OUT2</sub>      Ch 6 = Relay Switch      Ch 7 = Relay Coil Current



A. Ch 1 = IN1      Ch 2 = IN2      Ch 3 = V<sub>OUT1</sub>  
Ch 4 = V<sub>OUT2</sub>      Ch 6 = Relay Switch      Ch 7 = Relay Coil Current

**Figure 9-13. PWM driving for a single-coil latching relay with driving profile FORWARD → COAST → REVERSE → COAST**

**Figure 9-14. PWM driving for a single-coil latching relay with driving profile FORWARD → BRAKE → REVERSE → BRAKE**



A. Ch 1 = IN1      Ch 2 = IN2      Ch 3 = V<sub>OUT1</sub>  
Ch 4 = V<sub>OUT2</sub>      Ch 6 = Relay Switch      Ch 7 = Relay Coil1 Current  
Ch 8 = Relay Coil2 Current

**Figure 9-15. PWM driving for dual-coil relay**

### 9.2.4 Multi-Sourcing with Standard Motor Driver Pinout

The DRV8870, DRV8251, and DRV8231 devices come in an industry standard package footprint in the DDA package. When the system needs current sensing, a current-sense amplifier may be used across the R<sub>SENSE</sub> resistor to provide an amplified signal back to an microcontroller ADC as shown in [Figure 9-16](#). To reduce the size of the system bill of materials and cost, the IPROPI function in DRV8231A/51A can replace the current sense amplifier. During the board design process, both solutions, IPROPI and industry standard shunt devices, can be accommodated in the same board layout by placing and not placing (DNP) components as shown in [Figure 9-17](#). This allows the system to be flexible for lowest cost with the DRV8231A/51A or for use with second-source devices with the same pinout as DRV8870, DRV8231, and DRV8251.

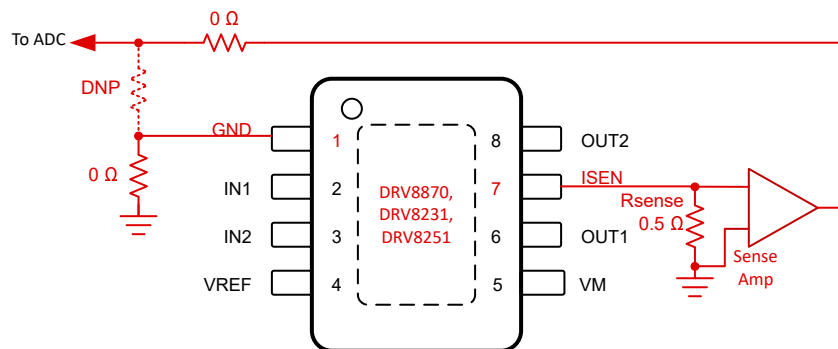


**Figure 9-16. Standard Pinout with Current Sense Amplifier**

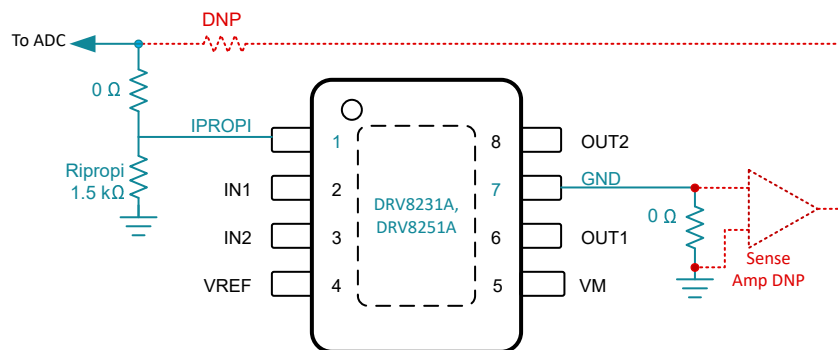


**Figure 9-17. DRV8231A/51A Device Using IPROPI to Integrate The Current Sense Function into The Motor Driver**

### 9.3 Current Capability and Thermal Performance

The output current and power dissipation capabilities of the driver depends heavily on the PCB design and external system conditions. This section provides some guidelines for calculating these values.

#### 9.3.1 Power Dissipation and Output Current Capability

Total power dissipation for the device consists of three main components: quiescent supply current dissipation ( $P_{VM}$ ), the power MOSFET switching losses ( $P_{SW}$ ), and the power MOSFET  $R_{DS(on)}$  (conduction) losses ( $P_{RDS}$ ). While other factors may contribute additional power losses, they are typically insignificant compared to the three main items.

$$P_{TOT} = P_{VM} + P_{SW} + P_{RDS}$$

$P_{VM}$  can be calculated from the nominal motor supply voltage ( $V_{VM}$ ) and the  $I_{VM}$  active mode current specification.

$$P_{VM} = V_{VM} \times I_{VM} \quad (4)$$

$$P_{VM} = 96 \text{ mW} = 24 \text{ V} \times 4 \text{ mA} \quad (5)$$

$P_{SW}$  can be calculated from the nominal motor supply voltage ( $V_{VM}$ ), average output current ( $I_{AVG}$ ), switching frequency ( $f_{PWM}$ ) and the device output rise ( $t_{RISE}$ ) and fall ( $t_{FALL}$ ) time specifications.

$$P_{SW} = P_{SW\_RISE} + P_{SW\_FALL} \quad (6)$$

$$P_{SW\_RISE} = 0.5 \times V_M \times I_{AVG} \times t_{RISE} \times f_{PWM} \quad (7)$$

$$P_{SW\_FALL} = 0.5 \times V_M \times I_{AVG} \times t_{FALL} \times f_{PWM} \quad (8)$$

$$P_{SW\_RISE} = 26.4 \text{ mW} = 0.5 \times 24 \text{ V} \times 0.5 \text{ A} \times 220 \text{ ns} \times 20 \text{ kHz} \quad (9)$$

$$P_{SW\_FALL} = 26.4 \text{ mW} = 0.5 \times 24 \text{ V} \times 0.5 \text{ A} \times 220 \text{ ns} \times 20 \text{ kHz} \quad (10)$$

$$P_{SW} = 53 \text{ mW} = 26.4 \text{ mW} + 26.4 \text{ mW} \quad (11)$$

$P_{RDS}$  can be calculated from the device  $R_{DS(on)}$  and average output current ( $I_{AVG}$ ).

$$P_{RDS} = I_{AVG}^2 \times (R_{DS(ON)}_{HS} + R_{DS(ON)}_{LS}) \quad (12)$$

$R_{DS(ON)}$  has a strong correlation with the device temperature. Assuming a device junction temperature of 85 °C,  $R_{DS(on)}$  could increase ~1.5x based on the normalized temperature data. The calculation below shows this derating factor. Alternatively, [Section 7.6](#) shows curves that plot how  $R_{DS(on)}$  changes with temperature.

$$P_{RDS} = 225 \text{ mW} = (0.5 \text{ A})^2 \times (300 \text{ m}\Omega \times 1.5 + 300 \text{ m}\Omega \times 1.5) \quad (13)$$

Based on the example calculations above, the expressions below calculate the total expected power dissipation for the device.

$$P_{TOT} = P_{VM} + P_{SW} + P_{RDS}$$

$$P_{TOT} = 374 \text{ mW} = 96 \text{ mW} + 53 \text{ mW} + 225 \text{ mW} \quad (14)$$

The driver's junction temperature can be estimated using  $P_{TOT}$ , device ambient temperature ( $T_A$ ), and package thermal resistance ( $R_{\theta JA}$ ). The value for  $R_{\theta JA}$  depends heavily on the PCB design and copper heat sinking around the device. [Section 9.3.2](#) describes this dependence in greater detail.

$$T_J = (P_{TOT} \times R_{\theta JA}) + T_A \quad (15)$$

$$T_J = 100 \text{ }^{\circ}\text{C} = (0.374 \text{ W} \times 40.4 \text{ }^{\circ}\text{C/W}) + 85 \text{ }^{\circ}\text{C} \quad (16)$$

The device junction temperature should remain below its absolute maximum rating for all system operating conditions. The calculations in this section provide reasonable estimates for junction temperature. However, other methods based on temperature measurements taken during system operation are more realistic and reliable. Additional information on motor driver current ratings and power dissipation can be found in [Section 9.3.2](#) and [Section 12.1.1](#).

### 9.3.2 Thermal Performance

The datasheet-specified junction-to-ambient thermal resistance,  $R_{\theta JA}$ , is primarily useful for comparing various drivers or approximating thermal performance. However, the actual system performance may be better or worse than this value depending on PCB stackup, routing, number of vias, and copper area around the thermal pad. The length of time the driver drives a particular current will also impact power dissipation and thermal performance. This section considers how to design for steady-state and transient thermal conditions.

The data in this section was simulated using the following criteria.

#### HSOP (DDA package)

**Table 9-5. Simulation PCB Stackup Summary for HSOP package**

Layer	2-layer	4-layer
Top Layer	HSOP footprint with 1- or 2-oz copper thickness. See <a href="#">Table 9-6</a> for copper area varied in simulation. Thermally connected with vias (2 vias, 1.2-mm spacing, 0.3-mm diameter, 0.025-mm copper plating) from HSOP thermal pad to bottom layer and internal ground plane (4-layer only).	
Layer 2, internal ground plane	N/A	1-oz copper thickness, 74.2 mm x 74.2 mm copper area, thermally connected to HSOP thermal pad through vias.
Layer 3, internal supply plane	N/A	1-oz copper thickness, 74.2 mm x 74.2 mm copper area, not connected to other layers.
Bottom Layer	Ground plane with 1- or 2-oz copper thickness. See <a href="#">Table 9-6</a> for copper area varied in simulation. Thermally connected to HSOP thermal pad through vias.	1- or 2-oz copper thickness. Copper area fixed at 4.90 mm x 6.00 mm in simulation. Thermally connected to HSOP thermal pad through vias.

Figure 9-18 shows an example of the simulated board for the HSOP package. Table 9-6 shows the dimensions of the board that were varied for each simulation.

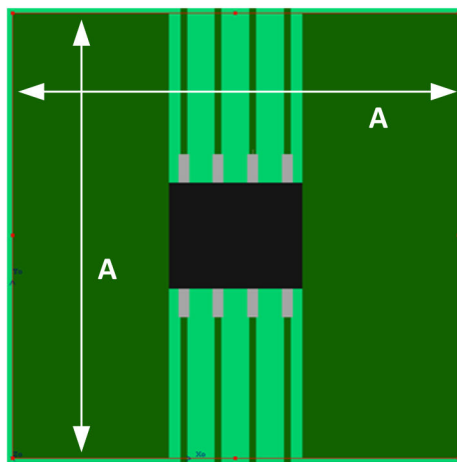


Figure 9-18. HSOP PCB model top layer

Table 9-6. Dimension A for 8-pin HSOP (DDA) package

Cu area ( $\text{cm}^2$ )	Dimension A (mm)
0.069	Package thermal pad dimensions
2	16.40
4	22.32
8	30.64
16	42.38

### WSON (DSG package)

Table 9-7. Simulation PCB Stackup Summary for WSON package

Layer	2-layer	4-layer
Top Layer	WSON footprint with 1- or 2-oz copper thickness. See Table 9-8 for copper area varied in simulation. Thermally connected with vias (2 vias, 1.2-mm spacing, 0.3-mm diameter, 0.025-mm copper plating) from WSON thermal pad to bottom layer and internal ground plane (4-layer only).	
Layer 2, internal ground plane	N/A	1-oz copper thickness, 74.2 mm x 74.2 mm copper area, thermally connected to HSOP thermal pad through vias.
Layer 3, internal supply plane	N/A	1-oz copper thickness, 74.2 mm x 74.2 mm copper area, not connected to other layers.
Bottom Layer	Ground plane with 1- or 2-oz copper thickness. See Table 9-8 for copper area varied in simulation. Thermally connected to WSON thermal pad through vias.	1- or 2-oz copper thickness. Copper area fixed at 2.00 mm x 2.00 mm in simulation. Thermally connected to WSON thermal pad through vias.

Figure 9-19 shows an example of the simulated board for the WSON package. Table 9-8 shows the dimensions of the board that were varied for each simulation.

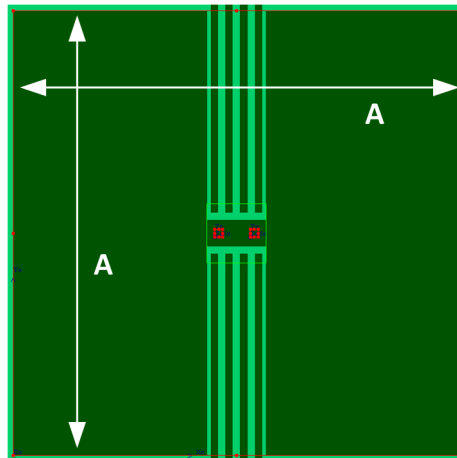


**Figure 9-19. WSON PCB model top layer**

**Table 9-8. Dimension A for 8-pin WSON package**

Cu area ( $\text{mm}^2$ )	Dimension A (mm)
0.015	Package thermal pad dimensions
2	15.11
4	20.98
8	29.27
16	40.99

### 9.3.2.1 Steady-State Thermal Performance

"Steady-state" conditions assume that the motor driver operates with a constant average current over a long period of time. The figures in this section show how  $R_{\theta JA}$  and  $\Psi_{JB}$  (junction-to-board characterization parameter) change depending on copper area, copper thickness, and number of layers of the PCB. More copper area, more layers, and thicker copper planes decrease  $R_{\theta JA}$  and  $\Psi_{JB}$ , which indicate better thermal performance from the PCB layout.

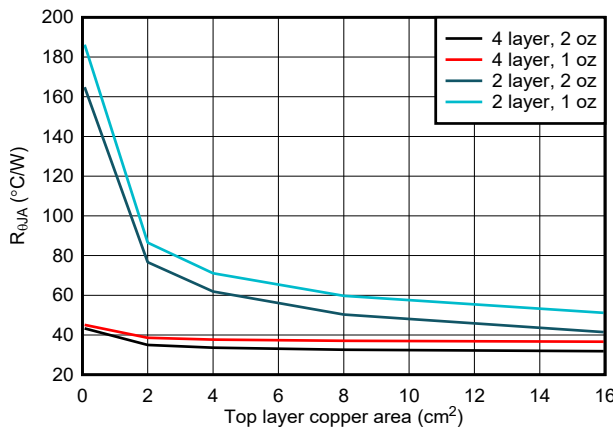


**Figure 9-20. HSOP, PCB junction-to-ambient thermal resistance vs copper area**

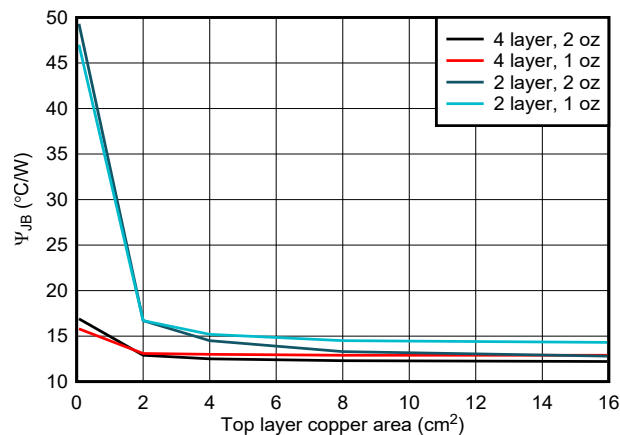


**Figure 9-21. HSOP, junction-to-board characterization parameter vs copper area**

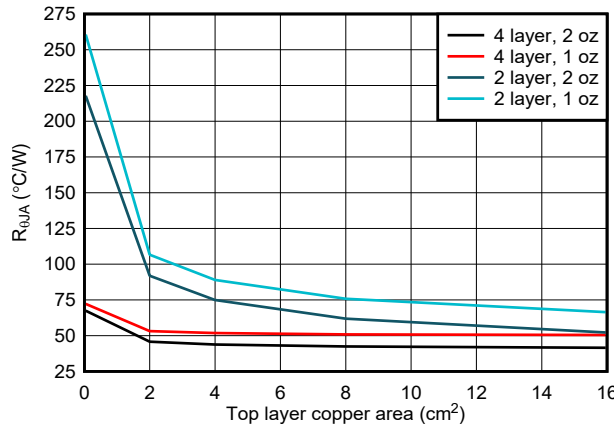


**Figure 9-22. WSON, PCB junction-to-ambient thermal resistance vs copper area**

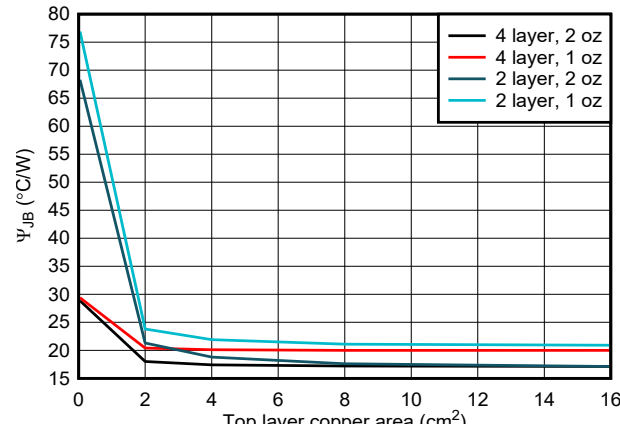


**Figure 9-23. WSON, junction-to-board characterization parameter vs copper area**

### 9.3.2.2 Transient Thermal Performance

The motor driver may experience different transient driving conditions that cause large currents to flow for a short duration of time. These may include

- Motor start-up when the rotor is initially stationary.
- Fault conditions when there is a supply or ground short to one of the motor outputs, and the overcurrent protection triggers.
- Briefly energizing a motor or solenoid for a limited time, then de-energizing.

For these transient cases, the duration of drive time is another factor that impacts thermal performance in addition to copper area and thickness. In transient cases, the thermal impedance parameter  $Z_{θJA}$  denotes the junction-to-ambient thermal performance. The figures in this section show the simulated thermal impedances for 1-oz and 2-oz copper layouts for the HSOP and WSON packages. These graphs indicate better thermal performance with short current pulses. For short periods of drive time, the device die size and package dominates the thermal performance. For longer drive pulses, board layout has a more significant impact on thermal performance. Both graphs show the curves for thermal impedance split due to number of layers and copper area as the duration of the drive pulse duration increases. Long pulses can be considered steady-state performance.

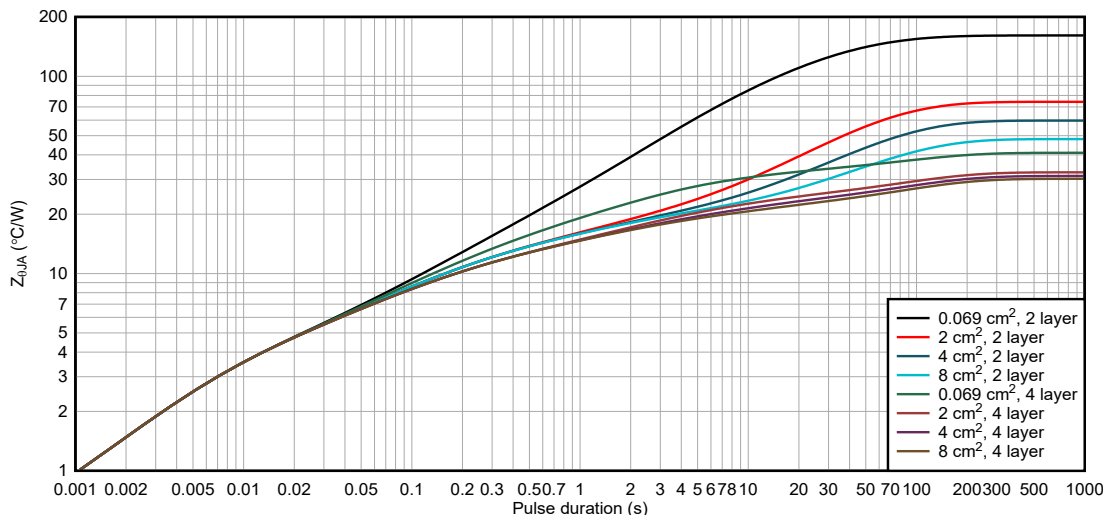


**Figure 9-24. HSOP package junction-to-ambient thermal impedance for 1-oz copper layouts**

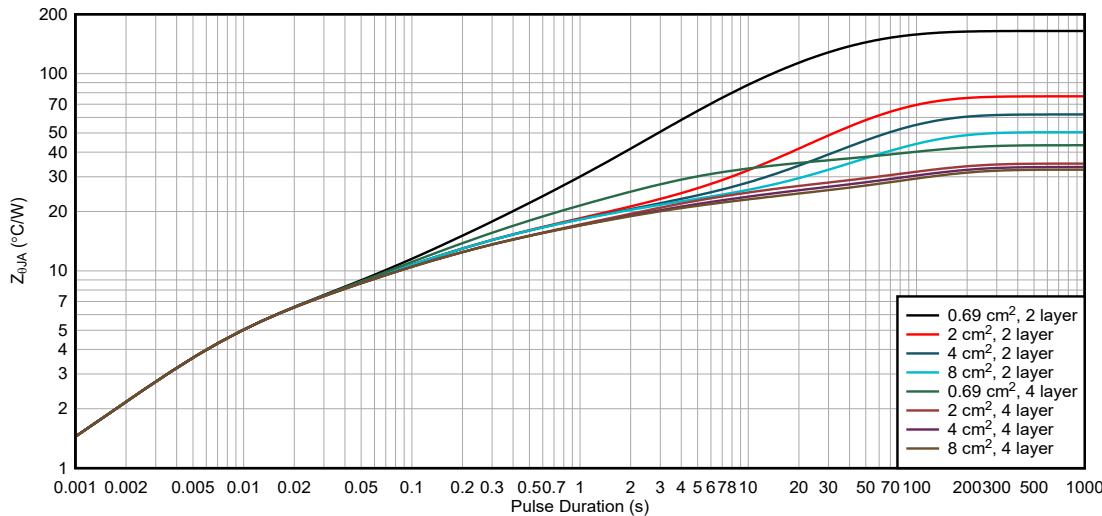


**Figure 9-25. HSOP package junction-to-ambient thermal impedance for 2-oz copper layouts**

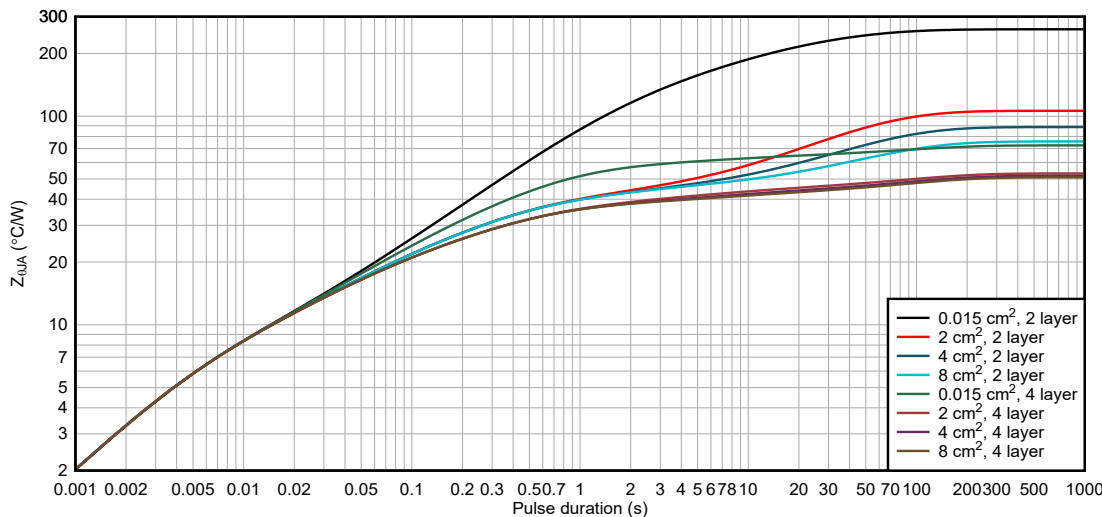


**Figure 9-26. WSON package junction-to-ambient thermal impedance for 1-oz copper layouts**

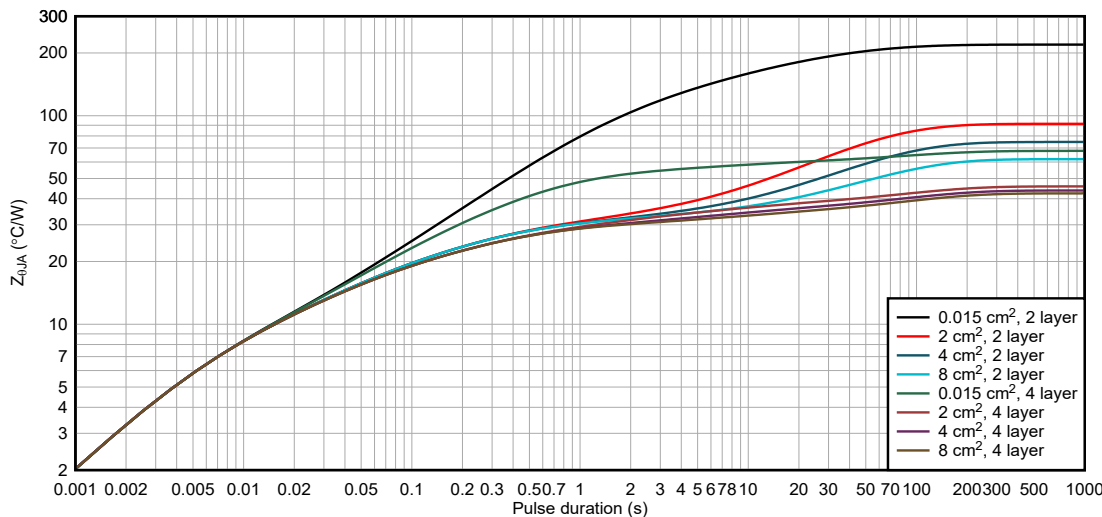


**Figure 9-27. WSON package junction-to-ambient thermal impedance for 2-oz copper layouts**

## 10 Power Supply Recommendations

### 10.1 Bulk Capacitance

Having appropriate local bulk capacitance is an important factor in motor drive system design. Having more bulk capacitance is generally beneficial, while the disadvantages are increased cost and physical size.

The amount of local capacitance needed depends on a variety of factors, including:

- The highest current required by the motor system
- The capacitance of the power supply and ability to source current
- The amount of parasitic inductance between the power supply and motor system
- The acceptable voltage ripple
- The type of motor used (brushed DC, brushless DC, stepper)
- The motor braking method

The inductance between the power supply and motor drive system limits how the rate current can change from the power supply. If the local bulk capacitance is too small, the system responds to excessive current demands or dumps from the motor with a change in voltage. When adequate bulk capacitance is used, the motor voltage remains stable and high current can be quickly supplied.

The data sheet generally provides a recommended value, but system-level testing is required to determine the appropriate sized bulk capacitor.

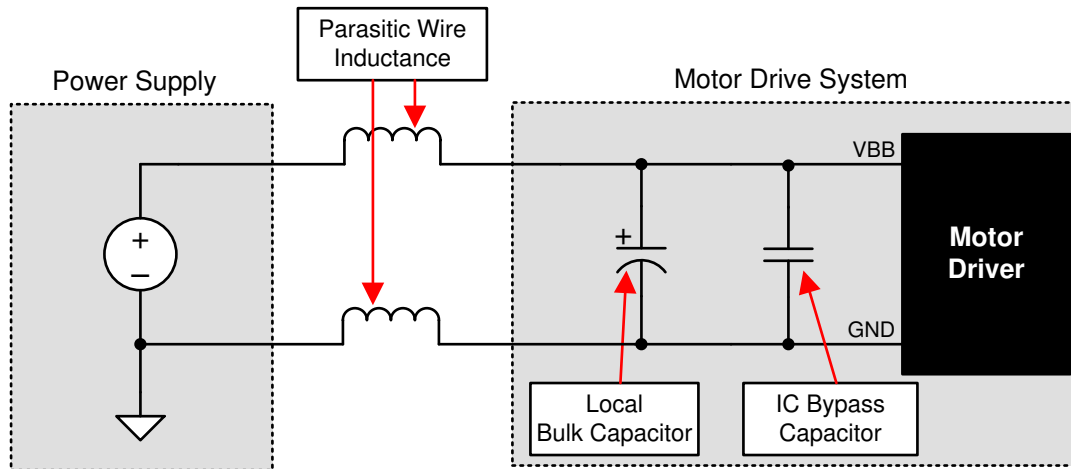


**Figure 10-1. Example Setup of Motor Drive System With External Power Supply**

The voltage rating for bulk capacitors should be higher than the operating voltage, to provide margin for cases when the motor transfers energy to the supply.

## 11 Layout

### 11.1 Layout Guidelines

Since the DRV8231A integrates power MOSFETs capable of driving high current, careful attention should be paid to the layout design and external component placement. Some design and layout guidelines are provided below.

- Low ESR ceramic capacitors should be utilized for the VM to GND bypass capacitor. X5R and X7R types are recommended.
- The VM power supply capacitors should be placed as close to the device as possible to minimize the loop inductance.
- The VM power supply bulk capacitor can be of ceramic or electrolytic type, but should also be placed as close as possible to the device to minimize the loop inductance.
- VM, OUT1, OUT2, and GND carry the high current from the power supply to the outputs and back to ground. Thick metal routing should be utilized for these traces as is feasible.
- The device thermal pad should be attached to the PCB top layer ground plane and internal ground plane (when available) through thermal vias to maximize the PCB heat sinking.
- A recommended land pattern for the thermal vias is provided in the package drawing section.
- The copper plane area attached to the thermal pad should be maximized to ensure optimal heat sinking.

### 11.2 Layout Example

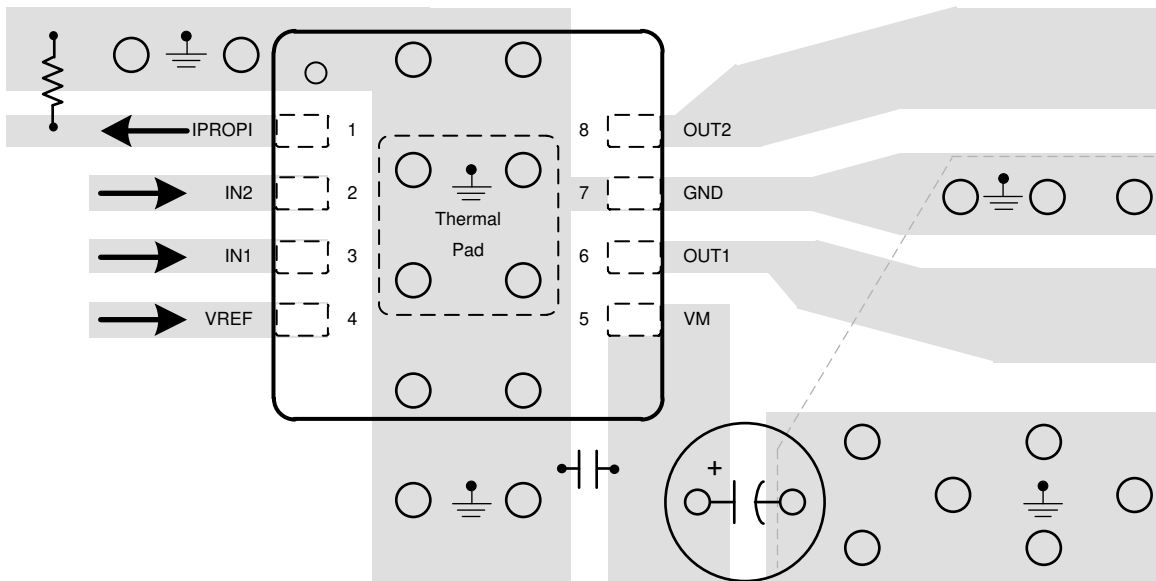


Figure 11-1. Layout Recommendation for DSG package

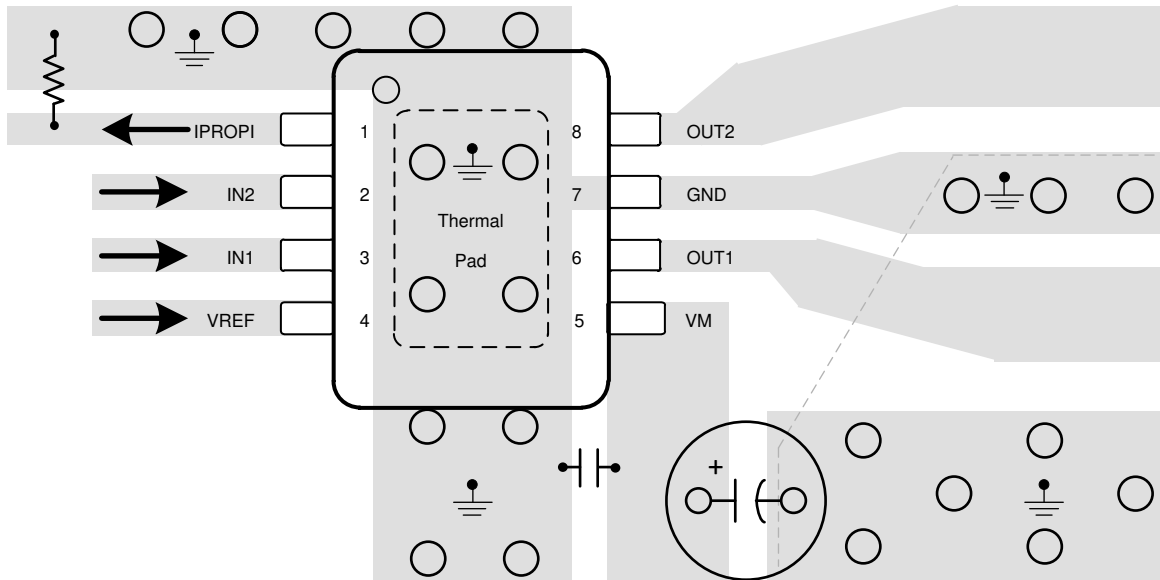


Figure 11-2. Layout Recommendation for DDA Package

## 12 Device and Documentation Support

### 12.1 Documentation Support

#### 12.1.1 Related Documentation

For related documentation, see the following:

- Texas Instruments, [Calculating Motor Driver Power Dissipation](#) application report
- Texas Instruments, [Current Recirculation and Decay Modes](#) application report
- Texas Instruments, [PowerPAD™ Made Easy](#) application report
- Texas Instruments, [PowerPAD™ Thermally Enhanced Package](#) application report
- Texas Instruments, [Understanding Motor Driver Current Ratings](#) application report

### 12.2 Receiving Notification of Documentation Updates

To receive notification of documentation updates, navigate to the device product folder on [ti.com](http://ti.com). In the upper right corner, click on *Alert me* to register and receive a weekly digest of any product information that has changed. For change details, review the revision history included in any revised document.

### 12.3 Community Resources

### 12.4 Trademarks

PowerPAD™ are trademarks of Texas Instruments.

All trademarks are the property of their respective owners.

## 13 Mechanical, Packaging, and Orderable Information

The following pages include mechanical, packaging, and orderable information. This information is the most current data available for the designated devices. This data is subject to change without notice and revision of this document. For browser-based versions of this data sheet, refer to the left-hand navigation.

**PACKAGING INFORMATION**

Orderable Device	Status (1)	Package Type	Package Drawing	Pins	Package Qty	Eco Plan (2)	Lead finish/ Ball material (6)	MSL Peak Temp (3)	Op Temp (°C)	Device Marking (4/5)	Samples
DRV8231ADDR	ACTIVE	SO PowerPAD	DDA	8	3000	RoHS & Green	NIPDAU	Level-3-260C-168 HR	-40 to 150	DRV8231A	Samples
DRV8231ADSGR	ACTIVE	WSON	DSG	8	3000	RoHS & Green	NIPDAU	Level-1-260C-UNLIM	-40 to 150	31A	Samples

(1) The marketing status values are defined as follows:

**ACTIVE:** Product device recommended for new designs.

**LIFEBUY:** TI has announced that the device will be discontinued, and a lifetime-buy period is in effect.

**NRND:** Not recommended for new designs. Device is in production to support existing customers, but TI does not recommend using this part in a new design.

**PREVIEW:** Device has been announced but is not in production. Samples may or may not be available.

**OBSOLETE:** TI has discontinued the production of the device.

(2) **RoHS:** TI defines "RoHS" to mean semiconductor products that are compliant with the current EU RoHS requirements for all 10 RoHS substances, including the requirement that RoHS substance do not exceed 0.1% by weight in homogeneous materials. Where designed to be soldered at high temperatures, "RoHS" products are suitable for use in specified lead-free processes. TI may reference these types of products as "Pb-Free".

**RoHS Exempt:** TI defines "RoHS Exempt" to mean products that contain lead but are compliant with EU RoHS pursuant to a specific EU RoHS exemption.

**Green:** TI defines "Green" to mean the content of Chlorine (Cl) and Bromine (Br) based flame retardants meet JS709B low halogen requirements of <=1000ppm threshold. Antimony trioxide based flame retardants must also meet the <=1000ppm threshold requirement.

(3) MSL, Peak Temp. - The Moisture Sensitivity Level rating according to the JEDEC industry standard classifications, and peak solder temperature.

(4) There may be additional marking, which relates to the logo, the lot trace code information, or the environmental category on the device.

(5) Multiple Device Markings will be inside parentheses. Only one Device Marking contained in parentheses and separated by a "~" will appear on a device. If a line is indented then it is a continuation of the previous line and the two combined represent the entire Device Marking for that device.

(6) Lead finish/Ball material - Orderable Devices may have multiple material finish options. Finish options are separated by a vertical ruled line. Lead finish/Ball material values may wrap to two lines if the finish value exceeds the maximum column width.

**Important Information and Disclaimer:** The information provided on this page represents TI's knowledge and belief as of the date that it is provided. TI bases its knowledge and belief on information provided by third parties, and makes no representation or warranty as to the accuracy of such information. Efforts are underway to better integrate information from third parties. TI has taken and continues to take reasonable steps to provide representative and accurate information but may not have conducted destructive testing or chemical analysis on incoming materials and chemicals. TI and TI suppliers consider certain information to be proprietary, and thus CAS numbers and other limited information may not be available for release.

In no event shall TI's liability arising out of such information exceed the total purchase price of the TI part(s) at issue in this document sold by TI to Customer on an annual basis.

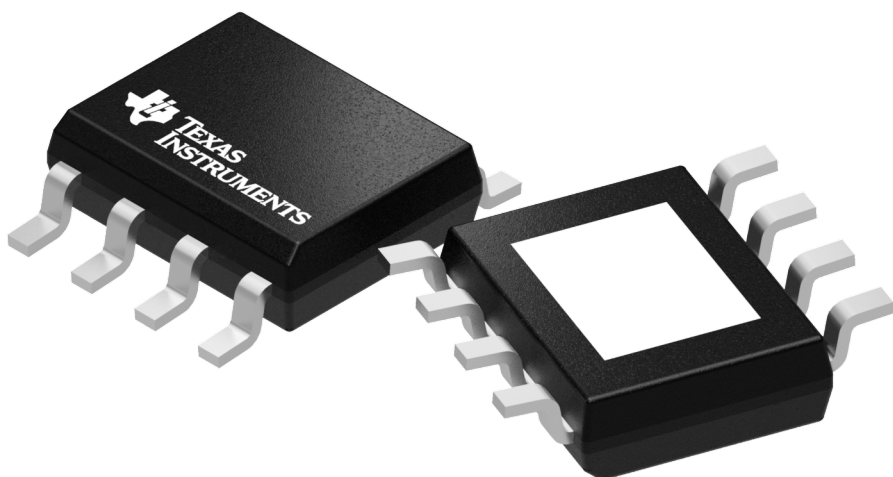


## GENERIC PACKAGE VIEW

DDA 8

PowerPAD™ SOIC - 1.7 mm max height

PLASTIC SMALL OUTLINE

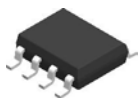


Images above are just a representation of the package family, actual package may vary.  
Refer to the product data sheet for package details.

4202561/G

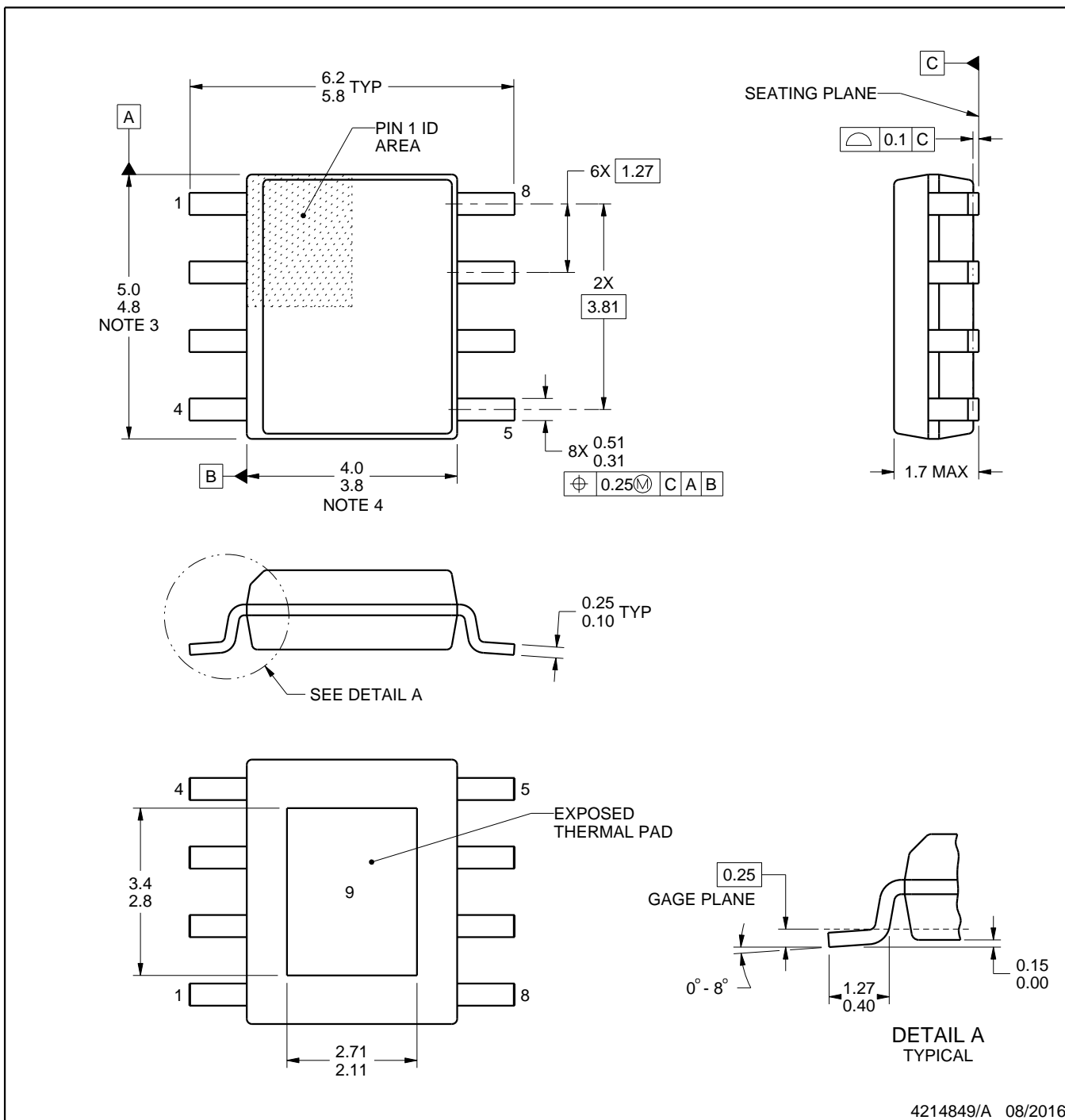
# PACKAGE OUTLINE

**DDA0008B**



**PowerPAD™ SOIC - 1.7 mm max height**

PLASTIC SMALL OUTLINE



4214849/A 08/2016

NOTES:

1. All linear dimensions are in millimeters. Any dimensions in parenthesis are for reference only. Dimensioning and tolerancing per ASME Y14.5M.
2. This drawing is subject to change without notice.
3. This dimension does not include mold flash, protrusions, or gate burrs. Mold flash, protrusions, or gate burrs shall not exceed 0.15 mm per side.
4. This dimension does not include interlead flash. Interlead flash shall not exceed 0.25 mm per side.
5. Reference JEDEC registration MS-012.

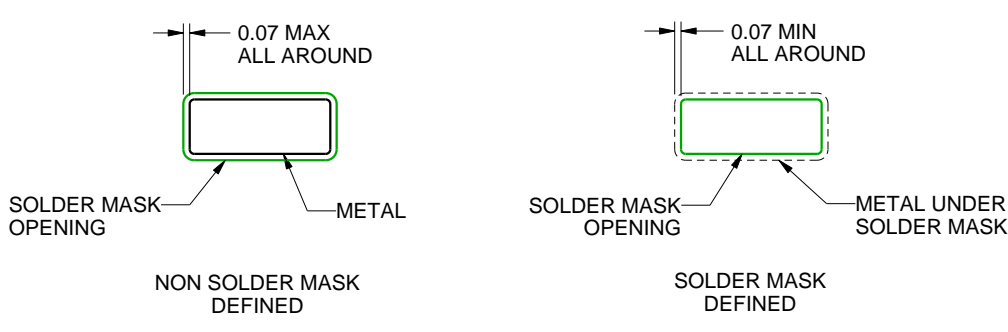
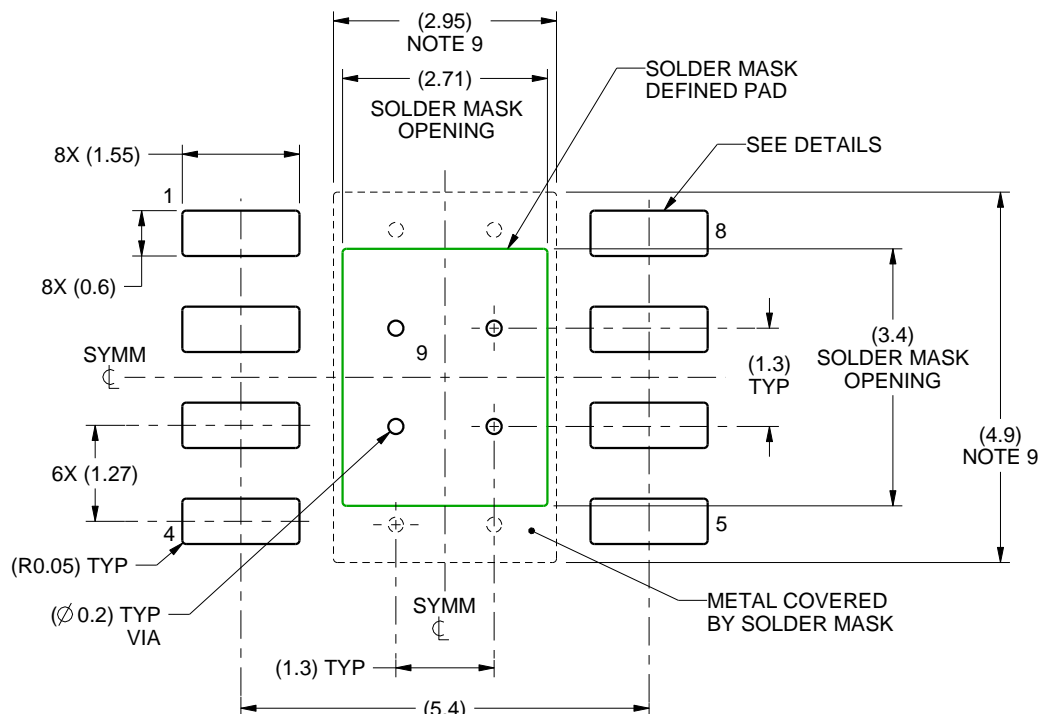
PowerPAD is a trademark of Texas Instruments.

# EXAMPLE BOARD LAYOUT

DDA0008B

PowerPAD™ SOIC - 1.7 mm max height

PLASTIC SMALL OUTLINE



4214849/A 08/2016

NOTES: (continued)

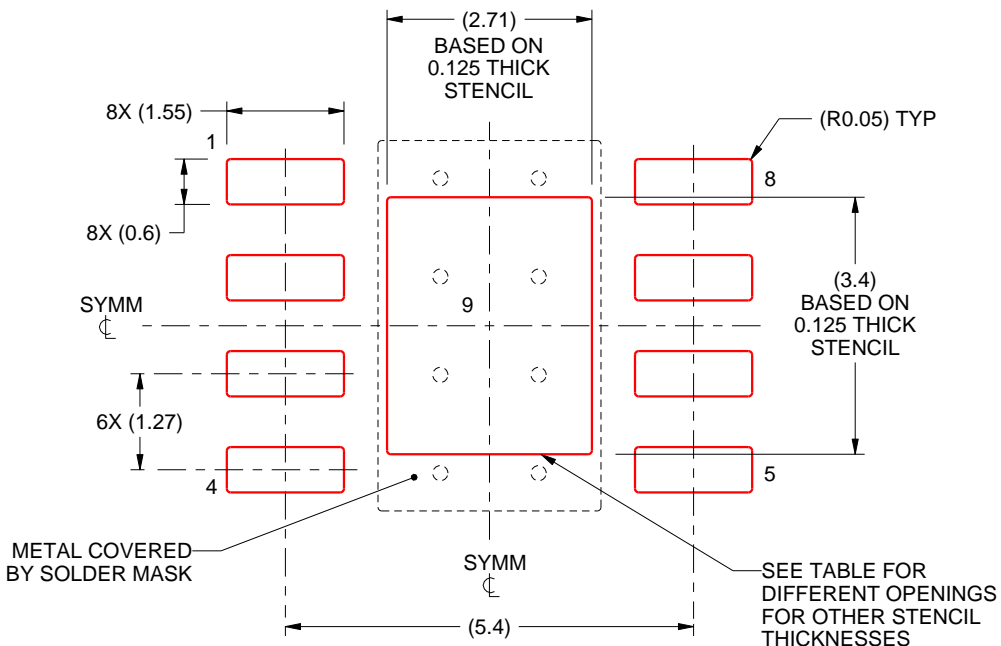
6. Publication IPC-7351 may have alternate designs.
7. Solder mask tolerances between and around signal pads can vary based on board fabrication site.
8. This package is designed to be soldered to a thermal pad on the board. For more information, see Texas Instruments literature numbers SLMA002 ([www.ti.com/lit/slma002](http://www.ti.com/lit/slma002)) and SLMA004 ([www.ti.com/lit/slma004](http://www.ti.com/lit/slma004)).
9. Size of metal pad may vary due to creepage requirement.
10. Vias are optional depending on application, refer to device data sheet. If any vias are implemented, refer to their locations shown on this view. It is recommended that vias under paste be filled, plugged or tented.

# EXAMPLE STENCIL DESIGN

DDA0008B

PowerPAD™ SOIC - 1.7 mm max height

PLASTIC SMALL OUTLINE



SOLDER PASTE EXAMPLE  
EXPOSED PAD  
100% PRINTED SOLDER COVERAGE BY AREA  
SCALE:10X

STENCIL THICKNESS	SOLDER STENCIL OPENING
0.1	3.03 X 3.80
0.125	2.71 X 3.40 (SHOWN)
0.150	2.47 X 3.10
0.175	2.29 X 2.87

4214849/A 08/2016

NOTES: (continued)

11. Laser cutting apertures with trapezoidal walls and rounded corners may offer better paste release. IPC-7525 may have alternate design recommendations.
12. Board assembly site may have different recommendations for stencil design.

## GENERIC PACKAGE VIEW

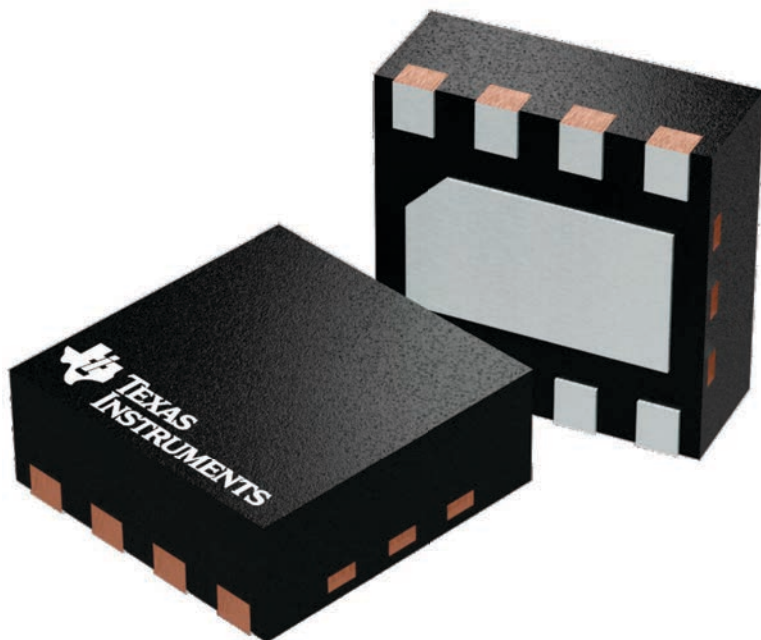
**DSG 8**

**WSON - 0.8 mm max height**

**2 x 2, 0.5 mm pitch**

**PLASTIC SMALL OUTLINE - NO LEAD**

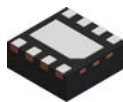
This image is a representation of the package family, actual package may vary.  
Refer to the product data sheet for package details.



4224783/A

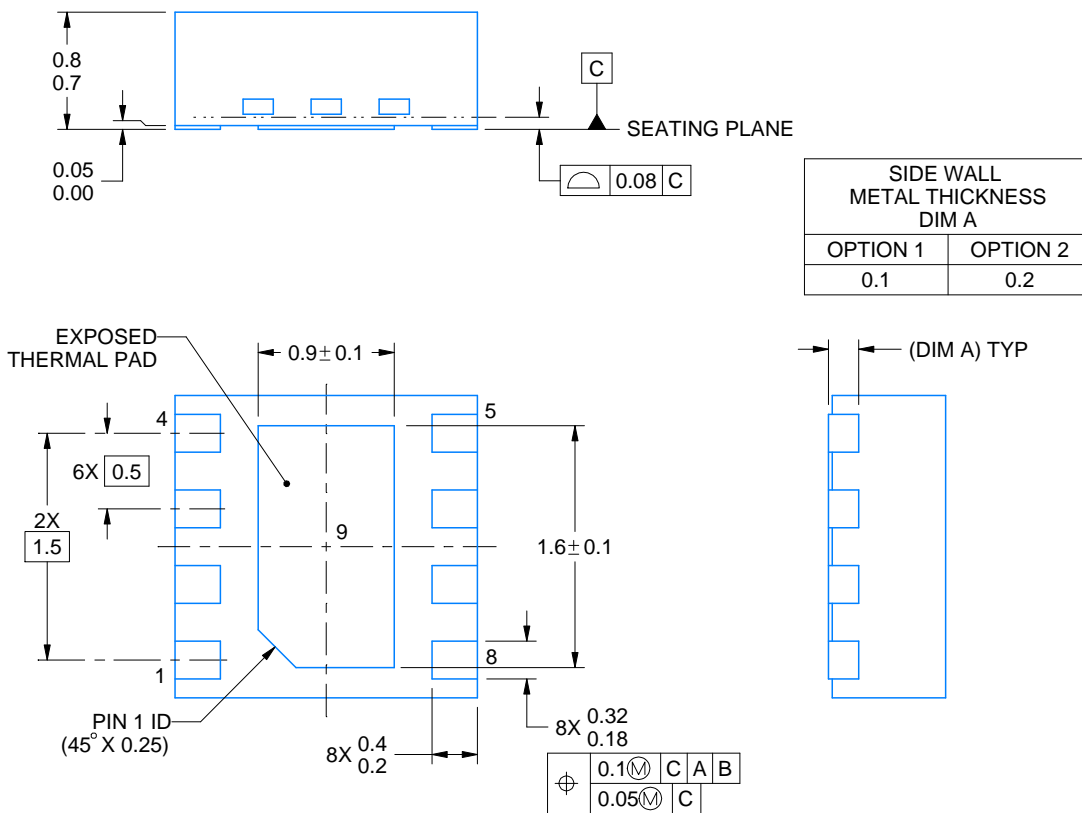
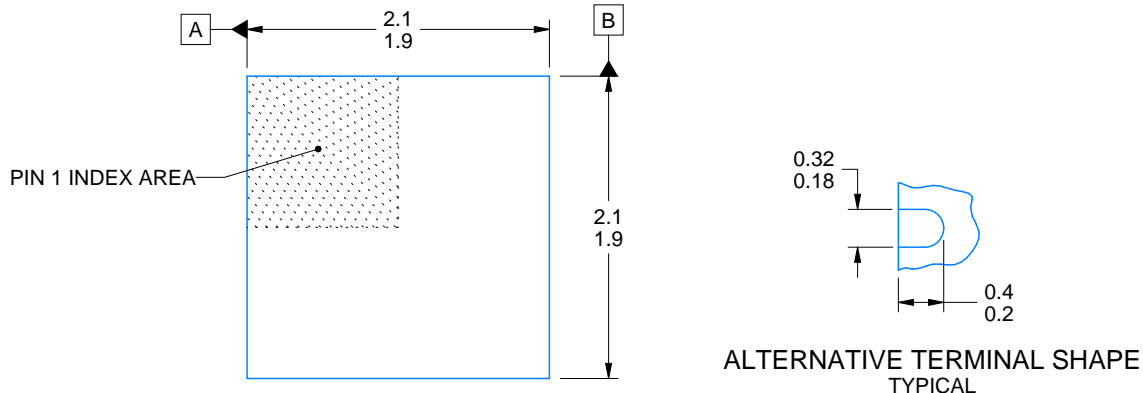
# PACKAGE OUTLINE

**DSG0008A**



**WSON - 0.8 mm max height**

PLASTIC SMALL OUTLINE - NO LEAD



4218900/E 08/2022

## NOTES:

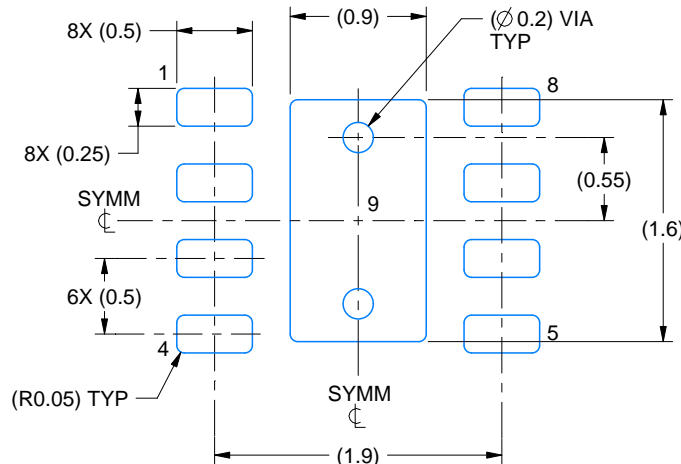
1. All linear dimensions are in millimeters. Any dimensions in parenthesis are for reference only. Dimensioning and tolerancing per ASME Y14.5M.
2. This drawing is subject to change without notice.
3. The package thermal pad must be soldered to the printed circuit board for thermal and mechanical performance.

# EXAMPLE BOARD LAYOUT

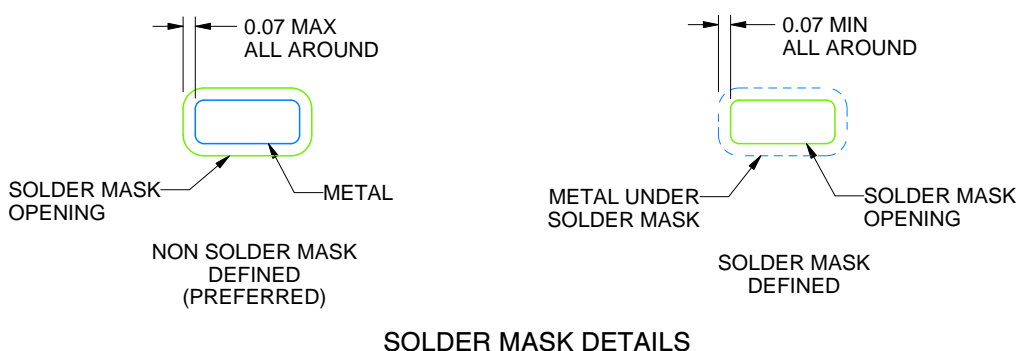
DSG0008A

WSON - 0.8 mm max height

PLASTIC SMALL OUTLINE - NO LEAD



LAND PATTERN EXAMPLE  
SCALE:20X



SOLDER MASK DETAILS

4218900/E 08/2022

NOTES: (continued)

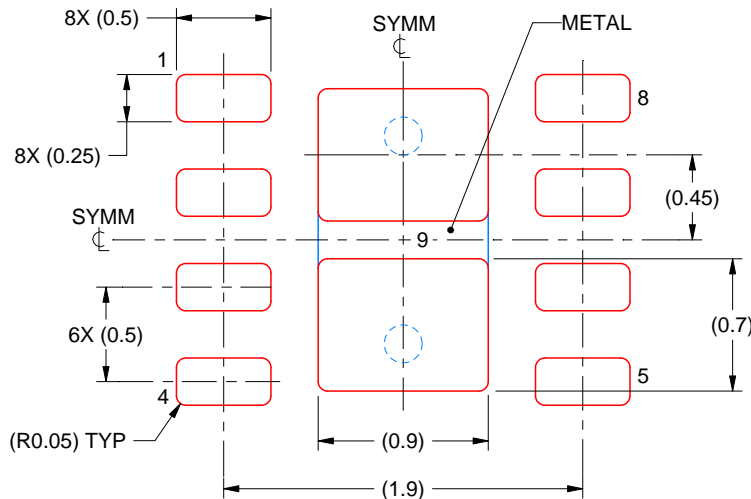
4. This package is designed to be soldered to a thermal pad on the board. For more information, see Texas Instruments literature number SLUA271 ([www.ti.com/lit/slua271](http://www.ti.com/lit/slua271)).
5. Vias are optional depending on application, refer to device data sheet. If any vias are implemented, refer to their locations shown on this view. It is recommended that vias under paste be filled, plugged or tented.

# EXAMPLE STENCIL DESIGN

DSG0008A

WSON - 0.8 mm max height

PLASTIC SMALL OUTLINE - NO LEAD



SOLDER PASTE EXAMPLE  
BASED ON 0.125 mm THICK STENCIL

EXPOSED PAD 9:  
87% PRINTED SOLDER COVERAGE BY AREA UNDER PACKAGE  
SCALE:25X

4218900/E 08/2022

NOTES: (continued)

6. Laser cutting apertures with trapezoidal walls and rounded corners may offer better paste release. IPC-7525 may have alternate design recommendations.

## **IMPORTANT NOTICE AND DISCLAIMER**

TI PROVIDES TECHNICAL AND RELIABILITY DATA (INCLUDING DATA SHEETS), DESIGN RESOURCES (INCLUDING REFERENCE DESIGNS), APPLICATION OR OTHER DESIGN ADVICE, WEB TOOLS, SAFETY INFORMATION, AND OTHER RESOURCES "AS IS" AND WITH ALL FAULTS, AND DISCLAIMS ALL WARRANTIES, EXPRESS AND IMPLIED, INCLUDING WITHOUT LIMITATION ANY IMPLIED WARRANTIES OF MERCHANTABILITY, FITNESS FOR A PARTICULAR PURPOSE OR NON-INFRINGEMENT OF THIRD PARTY INTELLECTUAL PROPERTY RIGHTS.

These resources are intended for skilled developers designing with TI products. You are solely responsible for (1) selecting the appropriate TI products for your application, (2) designing, validating and testing your application, and (3) ensuring your application meets applicable standards, and any other safety, security, regulatory or other requirements.

These resources are subject to change without notice. TI grants you permission to use these resources only for development of an application that uses the TI products described in the resource. Other reproduction and display of these resources is prohibited. No license is granted to any other TI intellectual property right or to any third party intellectual property right. TI disclaims responsibility for, and you will fully indemnify TI and its representatives against, any claims, damages, costs, losses, and liabilities arising out of your use of these resources.

TI's products are provided subject to [TI's Terms of Sale](#) or other applicable terms available either on [ti.com](#) or provided in conjunction with such TI products. TI's provision of these resources does not expand or otherwise alter TI's applicable warranties or warranty disclaimers for TI products.

TI objects to and rejects any additional or different terms you may have proposed.

Mailing Address: Texas Instruments, Post Office Box 655303, Dallas, Texas 75265  
Copyright © 2023, Texas Instruments Incorporated